M&B Technical Library

Electrical Engineering

Ferrites

E.E.Riches

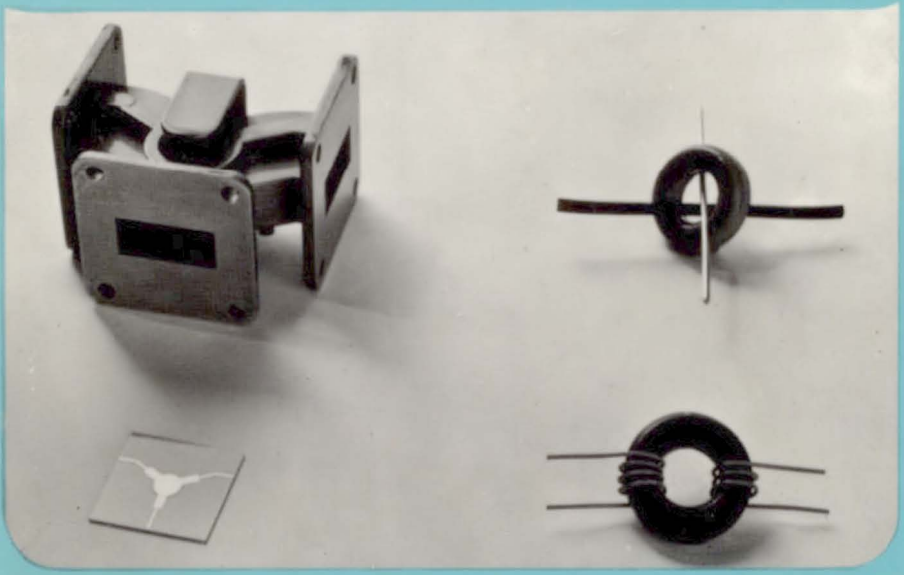

The Book

The development of ferrite materials has always been closely linked with their electronic engineering applications. This close association is followed in the book by relating each application to the properties of the preferred ferrites to provide an overall view of current technology.

After an introduction a short chapter outlines general methods of preparation of both single crystal and the more widely used polycrystalline ferrites. The various moderate-to-high permeability ferrites are then compared with regard to permeability loss and stability.

Properties of the hard ferrites used for permanent magnets are related to preparation and composition, as are the various ferrites used for computer memories. Developments in research on bubble domain devices are outlined which show potential applications for computer stores and digital signal processing.

The extensive use of ferrites at microwave frequencies is treated in terms of the physics of ferrimagnetic resonance. This leads to the many microwave devices which show non-reciprocal, or resonant properties. The related subject of magnetoelastic waves is reviewed, and microwave delay lines described. A final chapter details the properties of magnetostrictive ferrites used for electromechanical transducers.

ISBN 0 263. 05071. 8

£2.00 net

Other titles in this series

TL/EE/1 LINEAR ELECTRIC MOTORS
E R Laithwaite

TL/EE/2 AN INTRODUCTION TO THE JOSEPHSON EFFECTS
B W Petley

Other Electrical Engineering titles available

EE/1 THRESHOLD LOGIC
S L Hurst

EE/2 THE MAGNETRON OSCILLATOR
E Kettlewell

EE/3 MATERIAL FOR THE GUNN EFFECT
J W Orton

EE/4 MICROCIRCUIT LEARNING COMPUTERS
I Aleksander

EE/5 DC CONDUCTION IN THIN FILMS
J G Simmons

EE/6 READING MACHINES
J A Weaver

EE/7 SPEECH SYNTHESIS
J N Holmes

EE/8 GLOW DISCHARGE DISPLAY
G F Weston

EE/9 SUPERCONDUCTIVITY
I M Firth

All published by Mills & Boon Limited

M & B Technical Library TL/EE/3

General Editor: J Gordon Cook, PhD, FRIC

Ferrites

A Review of Materials and Applications

E E Riches, MSc

The General Electric Co Ltd

Mills & Boon Limited

London

First published in Great Britain 1972
by Mills & Boon Limited, 17–19 Foley Street
London, W1A 1DR.

ISBN 0 263.05071.8

Made and printed in Great Britain
by Butler & Tanner Ltd, Frome and London
Digitized and polished by PE1ABR

CONTENTS

Preface

Ferrites are now extensively used in electronic engineering by virtue of their high resistivity and consequently low eddy current and dielectric losses. They also find use in ceramic magnets which provide high magnetic fields in simple geometries at low cost. These applications of ferrites have resulted from intensive research and development over the past thirty years, during which time many thousands of papers and a number of specialized textbooks have been written on the subject. As yet, there is no indication of a reduction in the number of papers appearing each year; at the 1970 International Conference on Ferrites in Japan, for example, 174 papers were presented.

This proliferation of written papers is valuable and encouraging to the specialist, but deters the applied physicist or electronic engineer from obtaining a better understanding of particular ferrites or ferrite devices he wishes to use in the course of his work. The objective of this review is to provide this background by surveying the chemistry, physics and applications of ferrite materials. It is also intended to direct the reader to those selected references best suited to introduce the present state-of-the-art. For this reason few early papers are referenced, nor are their theories reproduced in detail. The reader who wishes to pursue a topic in depth will find the earlier papers from those referred to in the present text.

1. Introduction

Ferrites are iron oxide compounds usually containing at least one other metallic ion. The magnetic iron oxides Fe_3O_4 and Fe_2O_3, both of which are used in magnetic recording, are also usually included with the ferrites.[1] Table 1 lists the major structural groups of the ferrites together with their basic compositions. The Fe^{3+} ions in these may be replaced partially by the transition metals

Table 1. Crystal structures and chemical compositions of principal ferrites

CLASS OF FERRITE	CRYSTAL STRUCTURE	COMPOSITION
Spinels	Cubic spinel	$M^{2+}Fe_2^{3+}O_4$ where $M^{2+} = \left\{ \begin{matrix} Ni^{2+} \\ Mn^{2+} \\ Mg^{2+} \\ Zn^{2+} \\ Cu^{2+} \\ Co^{2+} \end{matrix} \right\}$ or mixtures
Garnets	Cubic garnet	$R_3^{3+}Fe_5^{3+}O_{12}$ where R^{3+} is a rare earth usually Y or Gd
Hexaferrite	Hexagonal magnetoplumbite	$BaFe_{12}O_{19}$ (M type) $Ba_2M^{2+}Fe_{12}O_{22}$ (Y type) $BaM_2^{2+}Fe_{16}O_{27}$ (W type) $Ba_3M_2^{2+}Fe_{24}O_{41}$ (Z type) $Ba_2M_2^{2+}Fe_{28}O_{46}$ (X type) $Ba_4M_2^{2+}F_{36}O_{60}$ (U type) where $M^{2+} = \left\{ \begin{matrix} Ni^{2+} \\ Co^{2+} \\ Zn^{2+} \\ Mg^{2+} \end{matrix} \right\}$ or mixtures
Orthoferrites	Orthorhombic perovskite	$R^{3+}Fe^{3+}O_3$ where R^{3+} is a rare earth or mixture of rare earths

Ni^{3+}, Mn^{3+}, Cr^{3+} or Co^{3+} and also by Al^{3+}, Ga^{3+} and V^{5+}. For most applications high resistivity is required to minimize eddy currents, or dielectric loss, in which case care must be taken during preparation to obtain stoichiometric compositions, or to make use of substitutions or additives which reduce electron hopping conductivity between adjacent ions in different valency states.[2] This is not important, however, in the case of the hexaferrites used for permanent magnets.

Table 2 gives the more important applications of these classes of ferrites.

Table 2. Major applications of ferrites

APPLICATION	CLASS OF FERRITE IN GENERAL USE
Magnetic cores for inductors and transformers	Spinels (up to 200 MHz) Planar hexaferrites (200–800 MHz)
Permanent magnets	Uniaxial hexaferrites
Microwave devices	Spinels Garnets (Hexaferrites)
Information storage	Spinels (including γFe_2O_3) (Single crystal orthoferrites and garnets)
Electromechanical transducers	Spinels
Magneto-elastic wave devices	Single-crystal garnets
Magneto-optic devices	Garnets

Some specialized applications use single crystals, but greater industrial use is made of the polycrystalline ceramic forms of ferrites. These ceramics are widely used because of their relative ease of manufacture combined with useful magnetic and insulating properties at normal temperatures; some are magnetic up to temperatures of 500°C or more.[3]

The spontaneous magnetization of the ferrites was ex-

plained by Néel in his classical theory of ferrimagnetism[4] in 1948. This theory has been treated by a number of authors; Reference 3, Chapter III, briefly summarizes Néel's work. The theory shows that ferrimagnetism is the general case of antiferromagnetism in which the spins of the magnetic ions are aligned and antiparallel in two (or more) interspaced sublattices. If the magnetic moments of the opposing sublattices are unequal then a net moment will result and the material is termed ferrimagnetic. When the moments are equal the resultant is zero and the material is antiferromagnetic. If the temperature is raised from 0 K a point is eventually reached above which the spontaneous magnetization is zero. This is named the *Curie point*. However, because the measured magnetic moment is the difference between two larger moments, each of which may show a different temperature dependence, then in some cases the moments may be equal (and opposite) at some other temperature below the Curie temperature. This is named the *compensation point*. A classic example of this occurs with the yttrium gadolinium garnets.[5]

The magnetic moments of the various magnetic ions which may be introduced into the ferrite lattices can be calculated.[6] By taking these in their molecular proportions for the particular ferrite it is possible to calculate the resulting magnetic moment. A special case arises when the strongly magnetic Fe^{3+} ion is replaced by a non-magnetic ion, usually aluminium Al^{3+}. Because of its size, the Al^{3+} tends to replace the Fe^{3+} in the sublattice with the greater magnetic moment. The resultant magnetic moment is thereby reduced. Unfortunately this also has the effect of reducing the Curie temperature, with a consequent increase of the temperature coefficient of magnetization about normal ambient temperatures.

Ferrites show macroscopic magnetic properties which are similar to those of the ferromagnetic metals such as iron, nickel, cobalt and their many alloys. The net magnetization is related to applied field by the classic hysteresis loop defined by the material parameters saturation magnetiza-

tion (B_S), remanence (B_{rem}), and coercivity (H_C). This characteristic arises from a closed magnetic domain structure in the single crystal grains of unmagnetized ferrite. These have been observed directly in single crystal ferrites[7] and, as in the ferromagnetic materials, they explain many of the properties of unmagnetized ferrites.

The spinels and garnets are soft ferrites with low coercivity. Some of these compositions, notably manganese–zinc ferrites and nickel–zinc ferrites, have very high permeabilities. The hexaferrites have generally high coercivities, being named hard ferrites by analogy with the permanent magnet steels.

2. Preparation of Ferrites

The mixed oxide process is used for the preparation of the bulk of polycrystalline ferrites for experimental and commercial applications. This has been described fully in a number of publications.[8, 9] The constituent metal oxides are mixed in a ball mill, initially fired to promote a partial reaction and finally ballmilled to a fine powder. This is then pressed to shape and finally fired at a high temperature (1200° to 1500°C) at which the particles sinter to a density of 95 to 99% or more of the theoretical density. This process varies in detail according to composition and application. The simplest control on composition and firing will yield usable hexaferrite magnets; on the other hand, certain garnets for microwave applications require control of composition to $\pm 0{\cdot}1\%$, with impurities at $<0{\cdot}02\%$. The more important aspects of this process are discussed in relation to applications in later sections of this review.

A number of other processes for preparing polycrystalline ferrites have been investigated. These are summarized in Table 3 with key references and some indication of areas of use. Apart from the mixed oxide process, only the process involving coprecipitation of insoluble oxalates or hydroxides has been used commercially. However, the arc plasma spray technique could become important if applications for ferrite films are exploited. The other methods all produce a powder which is subsequently sintered.

The final sintering process is the key to the control of magnetic properties. Detailed sintering mechanisms have been the subject of considerable research.[17, 18] Particle size distribution of the powder, its degree of reaction, impurities and their distribution, stoichiometry and homogeneity all affect the density, microstructure, and consequently magnetic properties of the final product. The wide use of the mixed oxide process is due to its being the

cheapest of those in Table 3; also, it is easily controlled. The mills and balls may be fabricated from iron (or iron alloys) and hence the iron pick-up may be allowed for in the starting composition. The pick-up for any new composition or prefiring condition must be determined experimentally for the mixed oxide process. The other processes do not have this disadvantage at the initial mixing stage. However, after prefiring, these processes require some form of comminution. If contamination by a ball milling stage is to be avoided, then the prefiring must be carried out using loose powder, or at low temperatures, so that the resulting cake pulverizes readily. This is often done in an air (or cyclone) mill, where the coarse prefired material mills upon itself in a high velocity air stream.[19]

Table 3. Basic methods for preparation of polycrystalline ferrites

METHOD	REFERENCE	APPLICATION OR CLASS FERRITE
Mixed oxide process	8, 9	All applications and classes of ferrites
Coprecipitation of insoluble oxalates or hydroxides	10	Spinels or garnets for most applications
Spray drying of mixed oxides or salts	11	Ferrites for experimental work, or wherever high purity and control of composition is required
Freeze drying of solutions of salts	12	As for spray drying above
Flame spraying	13	Microwave ferrites with fine grain size
Arc plasma	14	Thin film ferrites for memory or microwave applications
Fluidic bed reaction	15	Alternative to mixed oxide process
Electrolytic precipitation	16	Alternative to coprecipitation process

The second milling stage is not required if the ferrite powder is produced by the flame-spraying technique, as the product is then a fully reacted ferrite powder of extremely fine particle size. This is produced as a smoke by igniting the metal salts dissolved in an organic liquid such as alcohol which is burnt at high temperature in a gas flame. The subsequent precipitation of the fine ferrite particles in a cyclone separator may cause difficulties.

Table 4. Methods for preparing single crystal ferrites

METHOD	PROCESS	REFERENCE
Flux melt	The mixed oxides are dissolved in a suitable molten flux contained in a crucible which is then slowly cooled under controlled conditions. Single crystals seed and grow on the crucible walls.	20
Czochralski	A seed crystal is slowly pulled from a melt containing the dissolved oxides.	21
Verneuil or flame fusion	The ferrite powder is continuously sprayed onto a high temperature flame or plasma torch where it melts and deposits on a seed crystal as this is withdrawn from the flame.	22
Chemical vapour deposition	A vapour comprising a mixture of the component oxides produced in situ by chemical reaction is passed over a heated single crystal substrate where the ferrite is deposited directly from the vapour phase to give epitaxial growth.	23
Floating zone technique	A molten zone is slowly passed through a polycrystalline rod from a seed crystal at one end to progressively grow a single crystal.	24

Single crystals of all classes of ferrites are used in fundamental investigations of the materials and of magnetic processes. They are also used in specialized storage appli-

cations and at microwave frequencies. The many methods available for growth of ferrite crystals are discussed in Reference 1 (Chapter 2, Section 2), and the more important are given in Table 4. The most widely employed of these is the flux melt method,[20] in which a liquid is slowly cooled to grow the desired crystals. The fluxes used are often borates, or a mixture of lead oxide and lead fluoride. The latter has been particularly successful for growth of the rare earth iron garnets. High temperatures (1200–1400°C) must be used, requiring platinum crucibles, which are usually sealed to prevent vapour loss. The temperature is accurately controlled with a small gradient from top to bottom, and the crucible is cooled at 1–5°C/hr over periods of many days for growth of large perfect crystals. The chemical vapour deposition technique[23] for epitaxial growth of single crystal ferrite films is currently receiving attention as there are potentially important new applications for these. The process is complex and requires substrate crystals to be matched in thermal expansion characteristics as well as structure to prevent stress or cracking when the composite crystal is cooled to room temperature.

The detailed procedure used for preparing both single crystal and polycrystalline ferrites has important effects on their magnetic and dielectric properties. This is discussed further in the following sections in relation to their specific properties and applications.

3. Inductor Core Ferrites

The early development of polycrystalline ferrites was directed towards obtaining materials of high permeability and low loss for use in transformers and inductors. These provided an alternative to the high permeability silicon–iron and nickel–iron alloys which require laminating with thin layers of insulation for use at audio and higher frequencies. This work showed the superiority of manganese–zinc and nickel–zinc ferrites of spinel structure over other compositions. The superiority has been maintained over the past twenty years and these compositions account for nearly all ferrites prepared commercially for these and other applications summarised in Table 5.

Table 5. Principal applications of inductor core ferrites

APPLICATION	REQUIRED PROPERTIES	PREFERRED COMPOSITIONS
Transformers	High permeability $\mu = 10^4$ at 10 kHz $= 10^3$ at 10^2 kHz $= 10^2$ at 10 MHz $= 10$ at 500 MHz	MnZn ferrites for lower frequencies; NiZn ferrites for radio frequencies; planar hexaferrites at ultra-high frequencies
Inductors for filters and resonant circuits. Loading coils for cable circuits	Medium permeability i.e. $\mu = 2000$ up to 10^2 kHz Low loss Good stability Low distortion	MnZn ferrites for use up to 200 kHz; NiZn ferrites for use above 10^2 kHz
Recording heads for high-speed tape and disc recording	Moderate permeability at high flux levels. Good mechanical properties i.e. fine grain structure and freedom from pores	NiZn ferrites

The forms in which these cores are used are generally of two types, toroids (or ring) cores and pot cores (Figure 1).

The former are used mainly at radio frequencies, or where high permeability is required as in wide-band transformers. For most technical applications, however, the pot core is chosen for its compact size and good screening. This is now manufactured in diameters from 4 cm down to 12 mm, from which inductances from 5 H to a few μH may be obtained. The centre bosses of pot core halves may be gapped, reducing permeability to an effective value μ_{ett} and thus proportionally improving stability. A ferrite tuning core (or slug) is usually inserted in a hole through the centre boss. It is mounted on a screw thread such that its position in the air gap may be varied to alter the reluctance of the magnetic circuit, thus providing a small adjustment of the coil inductance. Other variants are the cross cores which are similar to pot cores, but have rectangular external form giving better packing density and access to the windings, and E and I sections used for applications such as line time–base transformers for TV receivers.

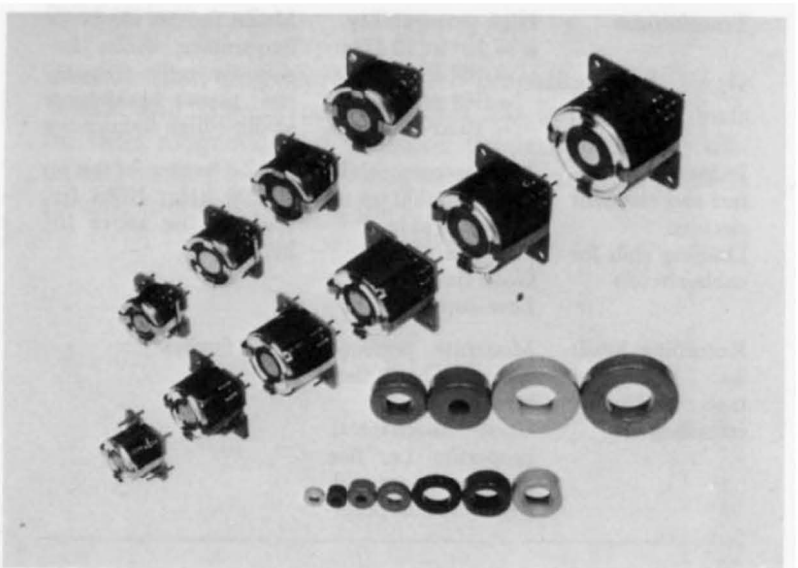

Fig. 1(a) *Range of pot cores and toroids.*

The range of compositions of the nickel–zinc and manganese–zinc ferrites, which may also incorporate certain metal oxide additives, is very large, as shown by the extensive literature and patents. These compositions have been developed to control some, or all, of the properties shown in Table 6, of which the most important is initial permeability μ measured on the unmagnetized ferrite (usually in the form of a toroid) with a small alternating

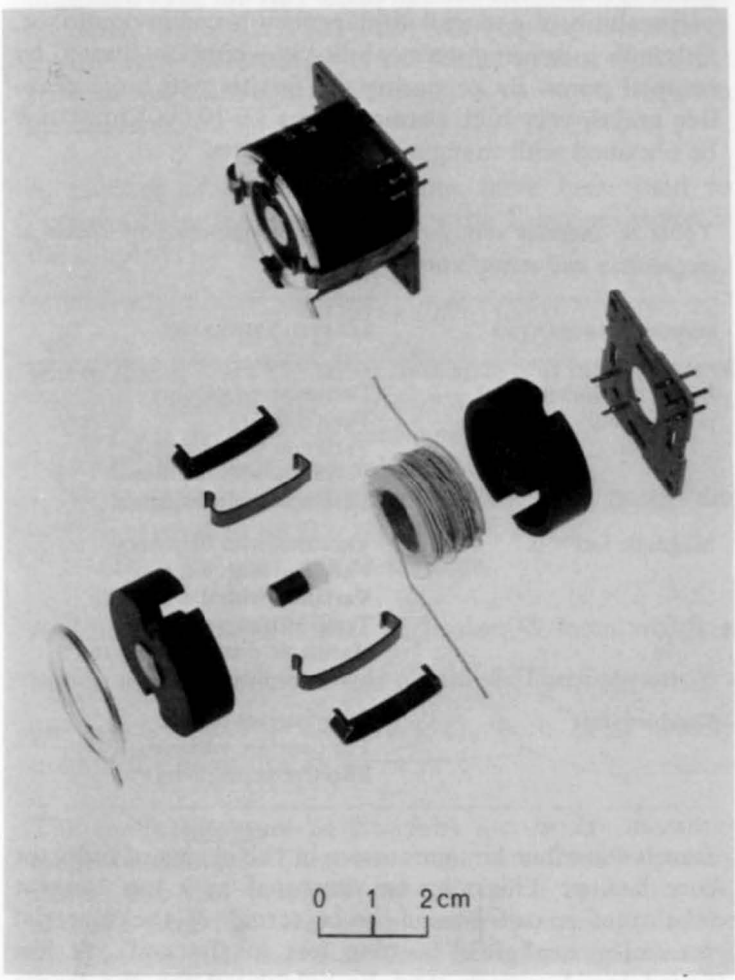

Fig 1(b) *Exploded view of ferrite pot core assembly.*

field of frequency f. This permeability is due to rotation of the spins within the domains of each crystalite of the ferrite ceramic into alignment with the applied field, and also to displacement of the domain walls.[25] The grain (or crystallite) size of the ferrite and the density of pores and non-magnetic inclusions within the grains will clearly effect the wall displacements and mobility. This has been investigated by Guillaud[26] who showed evidence that for grain size above about 5 μm in manganese–zinc ferrite the permeability due to wall displacement becomes dominant, although increasing permeability is eventually limited by trapped pores. By preparing the ferrite with large pore-free grains, very high permeabilities ($>$10,000) may now be obtained with manganese–zinc ferrites.

Table 6. Inductor core ferrite properties controlled by choice of composition and manufacturing process

PRINCIPAL PROPERTIES	RELATED PROPERTIES
Initial and incremental permeability	Temperature stability Time stability Variation with a.c. flux Variation with d.c. flux Variation with frequency
Magnetic loss	Variation with frequency Variation with a.c. flux Variation with d.c. flux Temperature variation Harmonic distortion due to hysteresis loss
Conductivity	Eddy current loss Temperature variation Effective permittivity

Loss is the other key parameter in the choice of inductor core ferrites. This may be measured as a loss tangent (tan δ) of a coil wound on a toroid of the material (assuming negligible resistive loss in the coil). A loss factor tan δ/μ may then be calculated for the ferrite material. This is a useful design parameter for the par-

ticular ferrite as the loss tangent of a gapped core is then $\left(\frac{\tan \delta}{\mu}\right) \times \mu_{\text{eff}}$.

The ferrite loss may be analysed into three components: the hysteresis loss, the eddy current loss, and a residual loss. The first arises from a loss in energy in traversing the hysteresis loop of the ferrite; this is small, but cannot be neglected even for very small applied fields as it produces harmonic distortion. The eddy current loss arises from conductivity mechanisms in the ferrite grains, whilst the residual loss is thought to be due to a variety of diffusion mechanisms.

A number of empirical relations have been used to evaluate these losses,[27] of which the Legg expression is the simplest:

$$\frac{R}{\mu f L} = C_h \hat{B} + C_e f + C_r$$

where R and L are the series resistance and inductance of a toroidal coil

C_h is the hysteresis coefficient

C_e is the eddy current coefficient

C_r is the residual loss coefficient (also partly dependent on f)

$\hat{B}$ is the peak flux in the core.

Another expression is that of Jordan[27] from which a hysteresis loss coefficient $\frac{h}{\mu^2}$ is obtained. These parameters are related by $h/\mu^2 = 1{\cdot}775 \times C_h$, both being widely used in the literature.

The coefficients may be found by a.c. bridge measurements of R and L. These are made at a fixed frequency but at two flux (i.e. coil current) levels to deduce C_h, and at a fixed flux level but at two frequencies to deduce C_e. The residual loss may then be calculated directly. Separation of the losses is useful in ferrite material development, as these are related to different aspects of the

physical and chemical structure. In addition, hysteresis loss is a measure of non-linearity at low fields; this is of particular interest to the applications engineer when designing circuits for which low harmonic level or low intermodulation distortion is required.

Although ferrites are generally considered to be insulators they have resistivities which may range from 10^3 ohm.m down to 1 ohm.m. Material with the lowest resistivity is of little use, other than for applications at very low frequencies. For radio frequency applications the resistivity must be high; for example, nickel–zinc ferrite has a resistivity $>10^3$ ohm.m. A special case is manganese–zinc ferrite, which has low resistivity within grains due to electron transfer between Fe^{2+} and Fe^{3+}. However, the boundary regions between grains can have a high resistivity, giving a relatively high bulk resistivity at d.c. When measured as a dielectric with a.c. an interesting effect is observed.[28] The permittivity reduces with increasing frequency, whilst the effective resistivity (measured as a dielectric loss) decreases. This arises from the capacitance of the bulk material being equivalent to two capacitances in series: that of the low resistivity large grains in series with the thin grain boundaries of high resistivity. Ferrites other than manganese–zinc ferrite show the effect to a lesser extent. This property has been used by Russian workers in temperature sensing elements, where the large fall in resistivity with increasing temperature (ρ to $10^{-2}\,\rho$ from 0 to 100°C) is exploited.[29]

The high effective permittivity ($\sim 10^5$) of manganese–zinc ferrites together with the high permeability ($\sim$2000) gives a very low velocity of e.m. wave propagation ($\sim 2 \times 10^4$ m.sec^{-1}). Thus standing waves, or dimensional resonances, may be excited in large pot cores at low radio frequencies, say 0·5 MHz. These will then absorb energy from the coil and lower its Q-factor at this frequency. It is therefore essential to keep the dimensions of manganese–zinc ferrite cores small for high frequency use.

Instability of permeability of inductor core ferrites has received particular attention. This is of two forms, firstly instability with changes in temperature, and secondly instability with time. Typical temperature-permeability characteristics of manganese–zinc and nickel–zinc ferrites are given in Figure 2. These show a permeability maximum close to the Curie temperature T_C and also secondary maximum at lower temperatures. The shapes of these curves is governed by composition and microstructure which are often modified to obtain controlled temperature coefficients of permeability close to room temperature.

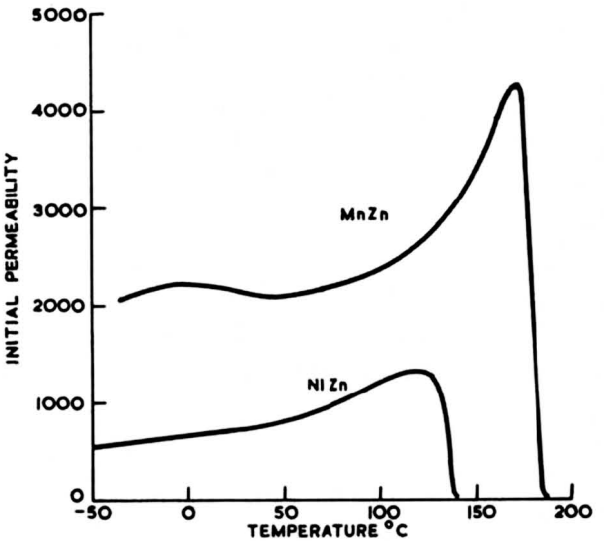

Fig. 2. Temperature-permeability characteristics of representative MnZn *and* NiZn *ferrites.*

Time instability, termed *disaccommodation*, has the form shown in Figure 3. The permeability relaxes, logarithmically with time such that

$$\frac{(\mu_1 - \mu_2)}{\log (t_1 - t_2)} \approx \text{const.}$$

The initial point at $t = 0$ is set by a magnetic, thermal or mechanical disturbance (or shock) which disturbs the configuration of domains within the crystallites. This

effect is normally quoted in terms of a disaccommodation factor

$$DF = \frac{(\mu_1 - \mu_2)}{\mu_1^2} \text{ per decade,}$$

i.e. between t and $10t$, where t is often chosen as 1 minute after the material is saturated and cyclically demagnetized by the field produced by a capacitor discharging through the coil.

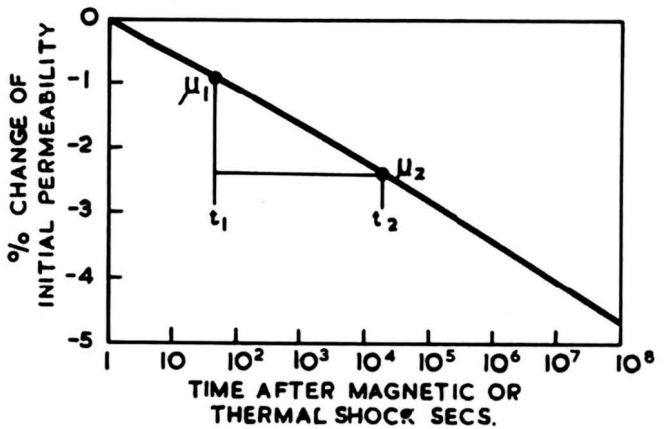

Fig. 3. Disaccommodation in MnZn *ferrite*

The explanation of disaccommodation in magnetic materials given by Snoek[30] may be divided into two parts; the effect of domain wall "stabilization" on the magnetization processes, and the mechanism by which the walls are stabilized. Snoek's analysis is still accepted from the former point of view, but the mechanism he proposed, a magneto-elastic effect, is now replaced by an ordering process appropriate to the material involved. Work by Iida[31] on cobalt ferrite supports the view that disaccommodation in spinel-structured ferrites (i.e. manganese–zinc and nickel–zinc ferrites) is due to vacancy migration causing changes in the induced magneto-crystalline anisotropy from point-to-point within the crystallites. The vacancy diffusion is related to preferential occupation by cations of certain lattice sites which are not equivalent with respect to the direction of magnetization.

The diffusion process will have a relaxation time varying with temperature for each type of cation diffusion and lattice parameter. This is shown clearly when disaccommodation of a toroid shocked by a d.c. saturating magnetic field is related to temperature[32] as in Figure 4. A series of maxima I to IV_{III} are seen in this particular manganese–zinc ferrite which has been fired and cooled in oxygen to increase vacancy concentration. These maxima are each caused by a particular diffusion mechanism. For example, Krupicka[33] suggests that the disaccommodation maximum in manganese ferrite close to room temperature has its origin in the direct interchange between Fe^{2+} ions and cation vacancies on neighbouring octahedral sites in the spinel lattice.

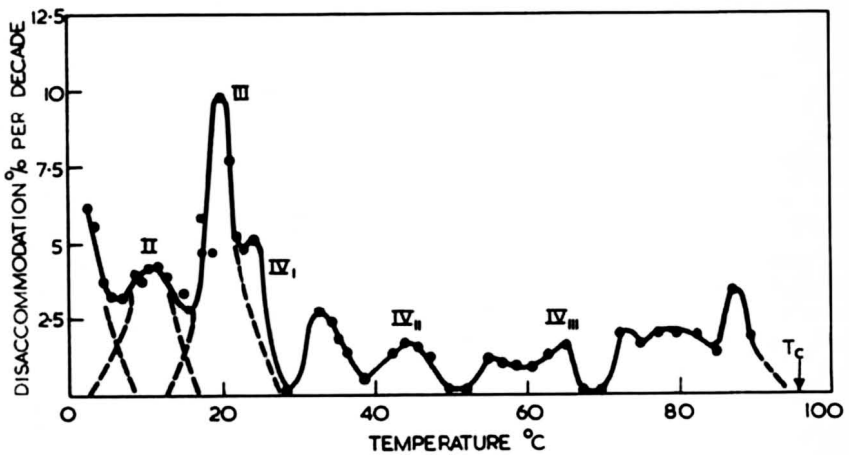

Fig. 4. Variation of disaccommodation with temperature of MnZn *ferrite cooled in air after sintering.*

3.1. NICKEL–ZINC FERRITES

Nickel ferrite $NiFe_2O_4$ has a spinel structure for which the magnetic moment arises from the opposed moments of Fe^{3+} ions in the tetrahedral sublattice and $Ni^{2+} + Fe^{3+}$ ions in the octahedral sublattice. The saturation magnetization is therefore fairly large at room temperature being 3,400 Gs (0·34 T) with a high Curie temperature (580°C).

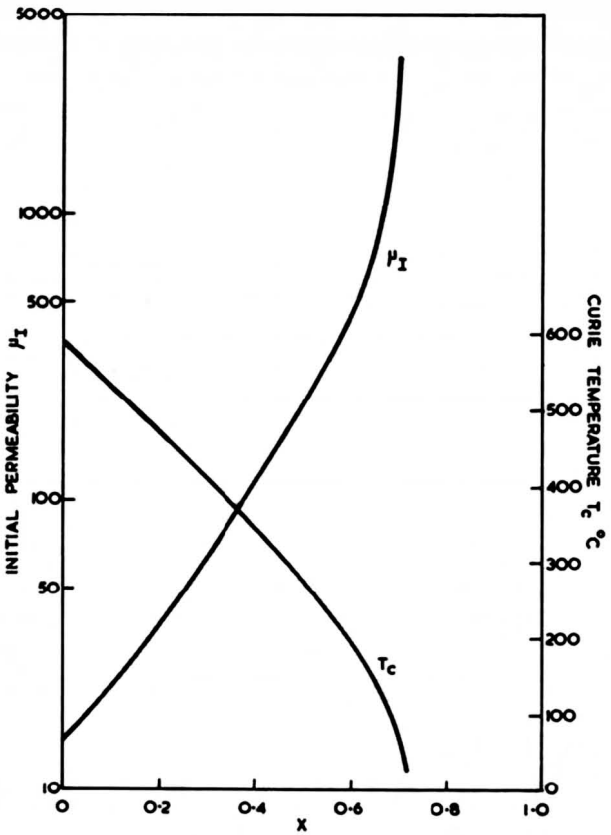

Fig. 5. (a) *Dependence of l.f. initial permeability at 20°C and Curie temperature on composition for* $Ni_{1-x}Zn_xFe_2O_3$.

The crystal anisotropy constant and magnetostriction are relatively high, whilst permeability is low ($\mu = 13$). If the Ni^{2+} is progressively replaced by non-magnetic Zn^{2+} the magnetic moment of the tetrahedral sublattice is reduced and the resultant magnetic moment increases. Eventually, the tetrahedral/octahedral coupling becomes so weak that the octahedral alignment is incomplete and the magnetic moment is reduced. The substitution of zinc for nickel also reduces the Curie temperature and raises the initial permeability just below the Curie temperature due to reduced magnetostriction and anisotropy.[34] This is illustrated in Figure 5(*a*), where permeability and Curie

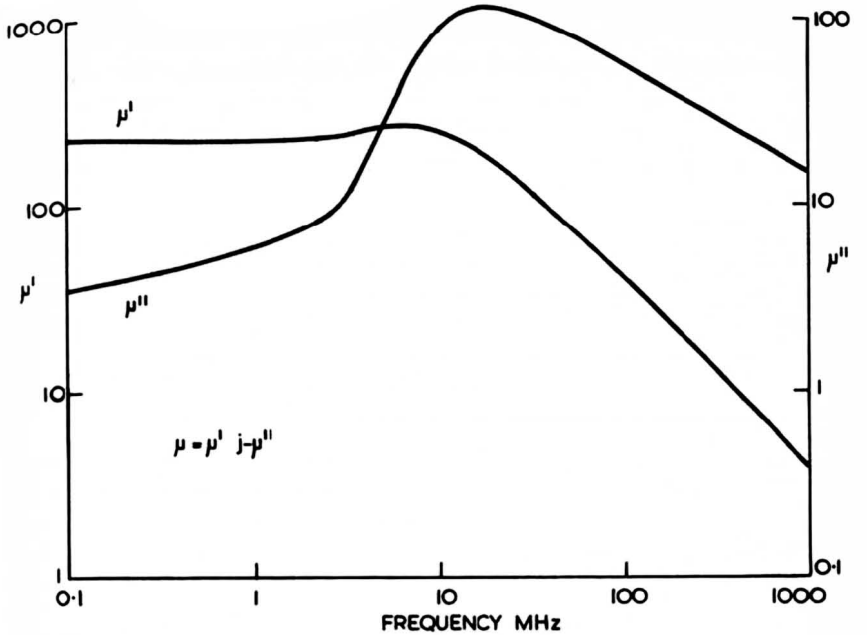

Fig. 5. (b) *Frequency dependence of complex initial permeability* μ *for* $Ni_{0.5}Zn_{0.5}Fe_2O_4$.

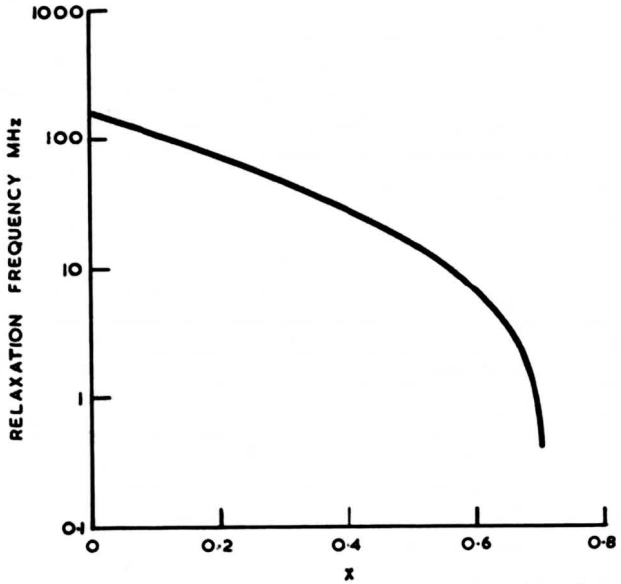

Fig. 5. (c) *Approximate variation of relaxation frequency with composition for* $Ni_{1-x}Zn_xFe_2O_3$.

temperature are related to composition. The actual value of permeability for any composition depends upon density and microstructure (including grain size) as already discussed.

If permeability and loss (measured as real and imaginary parts μ' and μ'' of the complex permeability) are plotted against frequency,[34, 35] characteristics such as given in Figure 5(*b*) are found. The reduction in μ' simultaneous with a peak in μ'' is due to domain wall resonances. At higher frequencies (>1 GHz) there is a second relaxation which arises from ferrimagnetic resonance (see Section 7.1). These domain wall resonances are not always observed.[35] Clearly, a particular composition should not be used close to or above the domain wall relaxation which defines a limiting frequency for use of each nickel–zinc composition as shown in Figure 5(*c*).

This range of compositions has been used commercially for many years in high frequency ferrites for r.f. coils, transformers and rod aerials. Recent research has been directed towards improving the μQ product together with temperature variation of permeability in the range 1 to 20 MHz. Improvements have been achieved by a small substitution (1%) of cobalt for (Ni_xZn_{1-x}) to produce a nickel–zinc–cobalt ferrite. Cobalt ferrite has a very large positive anisotropy constant K_1 compared with smaller negative values for the other spinel-structured ferrites. Thus a substitution of about 3% cobalt in the form of $CoFe_2O_4$ to nickel–zinc ferrite gives near zero anisotropy.[36] This reduces the loss, resulting in an improved μQ product. The cobalt substitution can also give a secondary maximum below room temperature in the μ-temperature characteristic, thereby modifying temperature stability over the normal operating range.

The cobalt substitution also reduces losses in non-stoichiometric nickel–zinc ferrite at high frequencies.[36]. This is believed to occur in these ferrites by stabilization of the domain walls by Co^{2+} because of its high anisotropy. In the case of iron-deficient material, the free electrons may

diffuse via Co^{2+} and Co^{3+} This occurs so quickly that any disturbance to the domain walls disappears with a short relaxation time and the walls are stabilized, thereby reducing losses. The stoichiometric ferrite does not have the free valence electrons, hence domain walls are not stabilized, giving high permeability but higher loss. The iron deficient nickel–zinc–cobalt ferrites must be fired in a strongly oxidizing atmosphere or the Co^{3+} will reduce to Co^{2+} and the electron-hopping mechanism will not occur and losses rise. The loss for these widely used ferrites may be further improved by preparing them with a fine grained microstructure.[37]

There is a specialized application of nickel–zinc ferrites requiring low porosity and controlled microstructure[38] in the magnetic cores of read–write heads for high speed digital tape or disc recording. These properties are necessary to allow machining of the ferrite and subsequent assembly of the heads to provide controlled gaps down to 1 μm in width.[39] The high density also gives good wear properties against the rapidly moving tapes with their abrasive coating of iron oxide. Recent work has been directed towards replacing the polycrystalline nickel–zinc ferrite with single crystal material in this application.[40]

3.2. MANGANESE–ZINC FERRITES

The other commercially important inductor core material is spinel-structured manganese–zinc ferrite having excess iron which enters the lattice as Fe^{2+} and Fe^{3+}. This may be more precisely described therefore as manganese–zinc ferrous ferrite. Compositions of this family may be prepared having permeabilities ranging from low values to more than 10,000 over a practical temperature range. This arises from the Fe^{2+} ions which cause the magnetocrystalline anisotropy constant K_1 to increase from a negative value at low temperatures to zero at around room temperature, above which it becomes positive but small, reducing again to zero at the Curie tempera-

ture.[41] The permeability temperature curves then show two maxima corresponding to the temperatures of zero anisotropy (Figure 6). The magnetostriction of these ferrites is also small due to positive magnetostrictive contribution of the Fe^{2+} ion in the lattice.[33] Near zero anisotropy and magnetostriction allow free rotation of spins to follow the applied alternating field, and also give high domain wall mobility, both leading to high permeability at audio, and low radio, frequencies with minimal hysteresis loss.

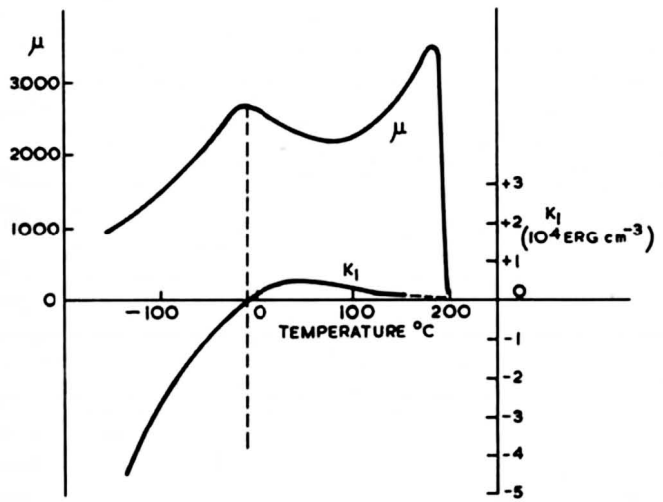

Fig. 6. Permeability and magnetocrystalline anisotropy constant K_1 *as a function of temperature for manganese-zinc ferrous ferrite.*

Microstructure of the manganese–zinc ferrites is very important in its effect on permeability and loss. Large pore-free grains give high permeability[42]; values of up to 40,000 have been reported for experimental and 10,000 for production materials. However, loss factor rises with increasing permeability due to relaxation losses occurring at lower frequencies, in addition to higher eddy current loss due to the larger grains. The latter loss is often minimized by preparing the ferrite to have insulating grain boundaries (small additions of calcium oxide and

silicon dioxide are sometimes employed for this purpose[43]), but high within-grain conductivity has to be accepted due to electron-hopping conductivity between the Fe^{2+} and Fe^{3+} ions. For this reason, those compositions required to have low losses usually have small grain size $\sim$6 μm giving moderate permeabilities $\sim$2000. The small grains then hold eddy current losses to low values. If these grains are also free from pores then hysteresis loss may be kept low.

As discussed earlier, disaccommodation must be minimized for certain applications where high stability is required. The technique adopted during the sintering of manganese-zinc ferrite to obtain the desired composition, i.e. all manganese and excess iron in the divalent state, is to fire in an optimum oxygen atmosphere and to cool in an equilibrium atmosphere.[44] This requires a controlled reduction of oxygen level during cooling, carried out by adjusting the flow of nitrogen to flush the kiln if this is of the simple type for firing individual batches.[44] It is now more common to sinter in a tunnel kiln in which the load is placed on tiles which are pushed through the heated zone of the kiln. Air and nitrogen are fed to the kiln to give an oxygen atmosphere in the high temperature zone, and a progressively lower oxygen level towards the cooler outlet.[45] This careful control of atmosphere is necessary to give low disaccommodation as excess oxygen will be taken up by the ferrite to give high concentrations of cation vacancies causing high disaccommodation.

Temperature stability is controlled mainly by choice of composition,[46] as this determines the Curie temperature and the general position of the secondary maximum (Figure 6). The firing conditions and atmosphere control are also important in determining the microstructure (grain size and intragranular porosity) and ferrous iron content. These both give a further control of the temperature of the permeability maxima and the width of these.

Another means for controlling permeability-temperature characteristics in manganese–zinc ferrite, whilst reducing eddy current loss, is to substitute tetravalent titanium for trivalent iron at levels of 5 mol%. Recent work[47] has suggested that a better control may be obtained by keeping the Fe^{2+} concentration constant and simultaneously increasing the Mn^{2+} and Ti^{4+} content whilst reducing the Fe^{3+}. (This gives compositions such as

$$Mn^{2+}_{0\cdot59+x}Zn^{2+}_{0\cdot3}\ Fe^{2+}_{0\cdot11}\ Ti^{4+}_{x}\ Fe^{3+}_{2-2x}O_4$$

where $x \sim 0\cdot05$ to $0\cdot10$.) Hysteresis loss is also reported to be low, giving total loss factor $\tan\delta/\mu = 1\cdot8 \times 10^{-6}$ at 100 kHz. This is similar to the best obtained with conventional manganese–zinc ferrite, but has the advantage of a linear μ-temperature characteristic between $-40°$ and 140°C.

It is evident that by these various techniques manganese–zinc ferrites may now be "engineered" to give any combination of permeability, loss (total, hysteresis and eddy current), disaccommodation and temperature stability suitable for a wide range of applications. The properties of many available inductor core ferrite materials are summarized in Reference 27, which also indicates the inductance and Q factors available for a wide range of core sizes and frequencies. Further information is available in manufacturers' data, but it is not easy to choose the best core for a particular requirement as Q factor depends upon the winding as well as the intrinsic properties of the ferrite. The increasing use of computer programmes to optimize coil design will help to remove this remaining problem for the electronic engineer.

3.3. HEXAGONAL FERRITES

The hexagonal-structured ferrites widely used for ceramic permanent magnets (Section 4) have high anisotropy, which has the effect of raising the ferromagnetic resonance frequency. The initial permeability is then maintained up to this very high frequency. Workers in the Philips

Laboratories in Holland showed[48] some years ago that in the case of hexagonal ferrites having planar anisotropy (that is to say the axis of easy magnetization lies anywhere within a plane normal to the hard direction) the permeability may be in excess of 10 up to 1000 MHz; on the other hand, a spinel ferrite of comparable permeability (nickel ferrite) shows the onset of ferromagnetic resonance relaxation at 150 MHz.

These materials are cobalt–zinc hexaferrites of composition $Co_xZn_{2-x}Ba_3Fe_{24}O_{41}$, for which the highest relaxation frequency but lowest permeability ($\mu = 10$) is found for $x = 2$. Alignment of the crystallites by pressing a slurry of single crystal particles of the ferrite in water in a rotating magnetic field prior to sintering gives an increased permeability ($\mu \sim 30$) without any significant lowering of the relaxation frequency. Another method of preparation using a topotactical reaction[49, 50] during sintering has been successfully used on some hexaferrites of planar anisotropy. This allows the simpler pressing in an axially applied field; the planar hexaferrite forms by chemical reaction during the sintering stage.

Planar hexaferrites are used in specialized applications such as balanced-unbalanced impedance matching transformers for U.H.F. television frequencies, and for pulse transformers.

4. Ferrite Magnets

The spinel-structured ferrites already discussed have a cubic close-packed structure of oxygen ions. A similar structure is hexagonal close-packed which may be combined with the cubic to form alternate layers of cubic and hexagonal co-ordination.[51] This structure is that of the mineral magnetoplumbite; it is also found in the synthetic oxide barium hexaferrite $BaFe_{12}O_{19}$, which has Fe^{3+} ions in three interstitial sites: tetrahedral and octahedral as in the spinels, and a site in which the ion is surrounded by five oxygen ions. The resultant magnetic moment of the ferrimagnetic ordering of these Fe^{3+} ions is high (20 Bohr magnetons/formula unit) corresponding to 4800 Gs (0·4T) at room temperature, and a Curie temperature of 450°C.

The unique property of the hexaferrites, however, is a high uniaxial magnetocrystalline anisotropy parallel to the c-axis of the single crystal. This c-axis is normal to the plane of the oxygen layers and may be easily identified in single crystals which readily cleave in planes normal to the c-axis and are often found as hexagonal platelets corresponding to the hexagonal structure. The anisotropy field of barium hexaferrite normal to the c-axis is close to 17,000 Oe ($1{\cdot}36 \times 10^6$ Am^{-1}), which gives rise to a high coercivity in polycrystalline barium hexaferrite.

The highest coercivities are found in polycrystalline material having a fine grain structure in which the crystallites are single domain. These crystallites of barium hexaferrite have the form of the natural plates with their c-axis normal to the plane. Calculations shows a single domain structure will occur for thickness of 1 μm or less. This is confirmed by progressively increasing the sintering temperature of barium hexaferrite compacts, which then show reducing coercivities from maximum values of 2000 Oe. The increasing density due to improved sintering raises the saturation magnetization, but domain structures

of adjacent crystallites interact thus further lowering coercivity. In practice, therefore, the optimization of the demagnetization characteristic of polycrystalline barium hexaferrite is critically dependent on both particle size of the starting material and sintering conditions.[52] Curves such as shown in Figure 7 are typical of those obtained with a fine-grain isotropic barium hexaferrite.

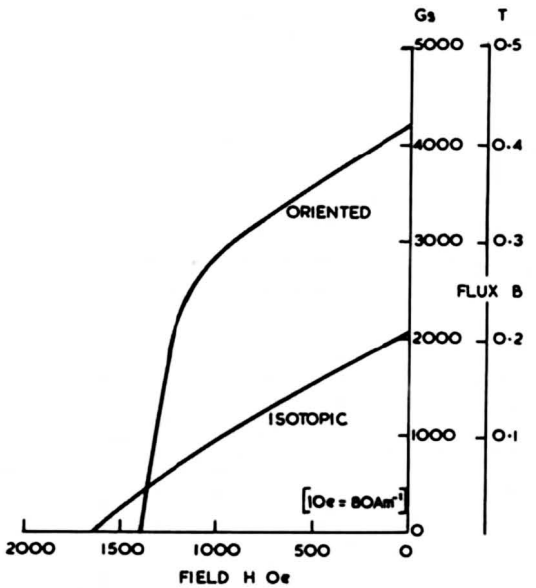

Fig. 7. Typical demagnetization curves of polycrystalline barium ferrite.

A further improvement of the permanent magnet properties is found by preparing polycrystalline barium hexaferrite with an aligned microstructure. The starting material is completely reacted barium hexaferrite ball-milled to single domain particle size (<1 μm). This is mixed with water and dispersing agents to form a thick slurry which is pressed in a high magnetic field along the pressing direction. The plate-like particles rotate under the action of the field and pressure to give an anisotropic compact with effective c-axis in the pressing direction.

The water present in the slurry is extruded from the com-

pact as the pressure increases and is removed via filter pads and fine holes in the pressing tool. The compact is then sintered to give a polycrystalline ceramic with properties approaching that of a single crystal. Remanence values of 3700 Gs (0·37 T) and $(BH)_{max}$ of 3×10^6 Gs Oe are obtained on production materials.

Both lead and strontium hexaferrites also have high magnetizations and anisotropy fields, but early work indicated that barium hexaferrite was superior to these. Extensive investigations of the three materials and their solid solutions by Cochardt[53, 54] in the mid-1960s showed that strontium hexaferrite could give higher energy products than barium hexaferrite, having values of up to $4{\cdot}8 \times 10^6$ Gs Oe which were obtained in production by introducing a small level of second phase impurities.[54] Magnet manufacturers now market both barium and strontium hexaferrites to provide a range of properties.

Ferrite magnets have lower remanence than modern alloy magnets (3800 Gs, cf 12000 Gs for Alnico) and are not therefore chosen for applications where high fields are of prime importance. The ferrites are, however, cheaper than the alloy magnets and have higher coercivities. Thus their applications tend to lie where the requirements are for cheap or compact forms of magnets. We find, for example, small discs of barium hexaferrite magnetized in repulsion being used to support the weight of the rotor of electricity meters to reduce wear in bearings, whereas large rings of 8 in diameter are used for high flux loudspeaker magnets. One of the most rapidly expanding applications is the use of ferrites in d.c. motors in automobiles. The cheap ferrite replaces expensive field windings of copper wire and lowers assembly costs. These magnets must be of aligned ferrite, for which techniques have been developed to radially align ferrite rings during pressing. Ferrite powder may also be permanently magnetized because of its high anisotropy, and is used extensively as a filler for rubber or plastics to provide a flexible magnetic material employed, for example, as a sealing strip for refrigerator doors.

Unlike alloy magnets, which have extremely good thermal stability, the hexaferrites have Curie temperatures of around 450°C and temperature stability of saturation magnetization of 0·2% per °C between ±100°C. The flux from a ferrite magnet will therefore vary with temperature of operation to a similar extent, although some stabilization may be obtained by temperature cycling before use.

5. Ferrite Core Memories

In the early 1950s it was shown that ferrite rings could be magnetized in either of the two directions around the ring to represent the binary digits "0" or "1". These states could be switched by current conductors threading the ring and the direction of magnetization sensed by a separate conductor in which an e.m.f. was induced on changing the remanent flux, the value of this e.m.f. indicating whether an "0" or "1" was stored. The rings or cores can be arranged in two-dimensional arrays (Figure 8) and individual cores selected by coincidence of current pulses of $I/2$ in wires threading the array in the x direction and $I/2$ in wires in the y direction. The practical arrangement of these systems is reviewed in Reference 55, while Reference 56 details present techniques for assembly of arrays having cores down to 0·014 in diameter.

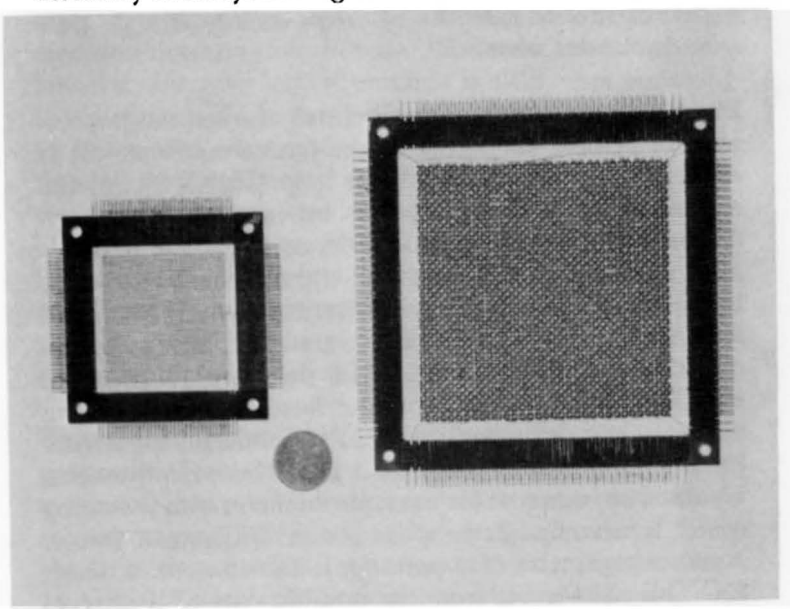

Fig. 8. Ferrite core memory planes containing 4096 cores; right: 0·050 in. dia. cores; left: 0·020 in. dia. cores. (Courtesy Mullard Ltd.)

Such memory stores, composed of up to $0{\cdot}5 \times 10^6$ cores, are used as immediate access stores of all types of electronic computers from the small desk machines to the largest centralized computers. The ferrite core memory of electronic computers is now a key component on which a considerable amount of technological research and development has been carried out during the past two decades.

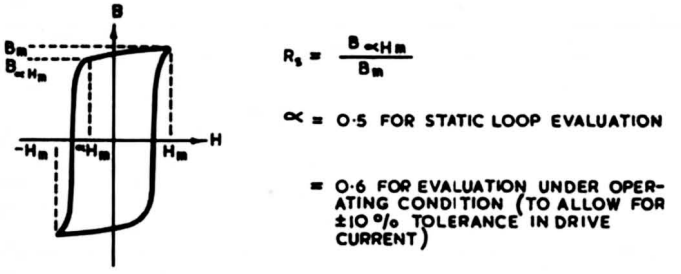

Fig. 9. Squareness ratio R_S *of ferrite memory core for 2 : 1 coincident current selection.*

Early work on switching cores clearly showed the importance of certain properties of the ferrite material: (*a*) it must have a "square" hysteresis loop (Figure 9), (*b*) the saturation magnetization must be large to give high output on switching, (*c*) coercivity must be low to minimize switching current, and (*d*) the switching time must be short. This last property is described by a merit factor S_w (Figure 10) which is equal to the ratio of the average distance domain walls move in the core to the wall mobility. The smaller is S_w the faster is the switching speed; values down to 0·5 Oe/μs are obtained for ferrites having grain sizes of less than 5 μm. These requirements are often opposing, as for example an increase in switching speed is accompanied by a poorer squareness factor. Another parameter of importance is known as delta noise: $\Delta\mu$. This noise arises from the non-linearity of the top of the hysteresis loop and is a measure of the noise output from the positive and negative half currents which thread cores not being switched.[57]

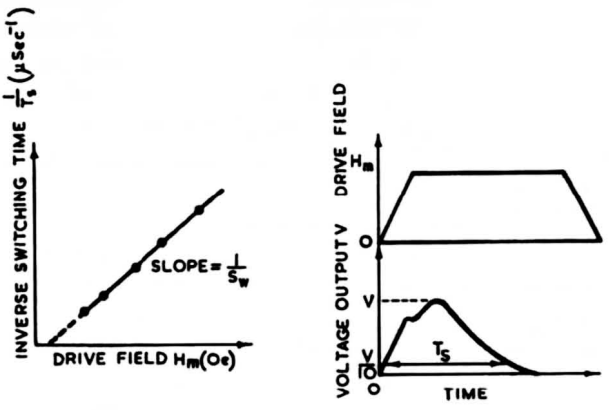

Fig. 10. Switching coefficient S_W *of ferrite core.*

These various characteristics have been considered in relation to the magnetic structure by a number of workers who have proposed models for the ideal switching core.[58] Wijn proposed that porosity and non-magnetic inclusions must be minimized, and magnetostriction in the easy direction must be close to zero. The stress anisotropy can, however, improve loop squareness if all stresses are along the direction of magnetization.[59] This was considered by Baltzer,[60] whose theory took account of the modification of magnetocrystalline anisotropy K_1 by magnetostriction. Other workers include the effect of distribution of magnetic inhomogeneities at which domain walls could be nucleated.[61] Present work favours the square loop requirement that magnetostriction should be zero, but that K_1 should not be zero (as is required, for example, in the high permeability inductor core ferrites).

The earliest ferrites to be found having these square loop properties were in the magnesium–manganese ferrite system. Compositions in this system are used extensively in microwave applications as discussed in Section 7.3, but the switching core ferrites have a greater manganese content, with typical compositions of $Mg_{0.85}Mn_{0.45}Fe_{1.7}O_4$. This ferrite must be cooled from the sintering temperature in nitrogen, as cooling in oxygen causes the Mn^{2+} to oxidize to Mn^{3+} giving the non-magnetic Mn_2O_3 com-

pound. An alternative approach which is sometimes adopted for these small toroidal cores is to rapidly quench down to room temperature from the sintering temperature.

The magnesium content affects K_1 and hence the coercivity. Experiments on partial substitution of zinc for magnesium were particularly effective giving H_c down to 0·6 Oe, with switching time S_w as low as 0·35 μs Oe. The smaller cores now used for high-speed stores require higher coercivities when drive current is increased to obtain faster switching. Thus for these a zinc substitution is disadvantageous. Recent work has been directed, therefore, to producing the magnesium–manganese ferrite compositions having fine grain size which reduces domain wall movement, thereby reducing S_w.

The manganese–copper ferrites have also found extensive use in switching core applications. Early work[62] reported properties of a composition $Cu_{0·25}Mn_{0·75}Fe_2O_4$, but addition of Mn_3O_4 was found to introduce Mn^{3+} ion into the lattice; this, together with the Cu^{2+} ion, improved loop squareness. The copper ferrite forms at relatively low temperatures and thereby assists control of grain size; however, it decomposes at close to 1150°C and care must be taken to control firing temperature and atmosphere.

Temperature stability of core materials has become more important as memory arrays have become larger and cycle time less. The latter trend has led to increased drive currents and greater power dissipation in the array, which is further exacerbated by increased size. Both the magnesium–manganese and manganese–copper ferrites have low Curie temperatures. This gives a rapid reduction of magnetization above room temperature, such that these materials may not be used above 70°C even with current compensation.[58] This problem is considerably reduced by use of lithium ferrites, which may operate at temperatures higher than 150°C by virtue of their high Curie temperature (640°C).

Lithium ferrite has the composition $Li_{0.5}Fe_{2.5}O_4$, in which the lithium ions are monovalent and the iron ions are all trivalent thus maintaining the valency balance. Early work on this ferrite showed that at temperatures below ~745°C the Li^+ and Fe^{3+} are ordered such that in the octahedral ion direction (110) there are necessarily three Fe^{3+} and one Li^+. At higher temperatures this structure is disordered, but the disorder may be quenched-in if the material is very rapidly cooled. The degree of disorder has been found to influence the hysteresis loop shape. The oxide Li_2O is volatile above 1100°C, and sintering must be carried out below this temperature, or precautions must be taken to reduce the loss of lithium. Excess lithium may be incorporated in the initial mix (usually in the form of lithium carbonate), or the cores may be flash-fired, i.e. taken rapidly up to and down from the sintering temperature.

Fine-grain lithium ferrite (2·5 μm) has S_w of 0·4 μs Oe and coercivity of 6 Oe, making it useful for fast storage applications. The squareness may be improved by certain additives of which Mn^{3+} is possibly the most important. This destroys the ordering of the structure, thereby affecting the K_1 and λ constants. There is, however, some disagreement in the literature as regards the role of order/disorder in obtaining high squareness ratios.[58]

Present developments have produced cores as small as 0·014 in outside diameter operated at cycle times as short as 0·5 μs. This cycle time probably could be halved again, but core apertures may not be reduced indefinitely as the wire size becomes too small to carry the switching currents. It is therefore possible that the economic limiting speed of ferrite cores has been or will soon be reached.

6. Bubble Domains

In 1967, Bobeck working at Bell Telephone Laboratories showed[63] that stable cylindrical magnetic domains (bubble domains) can be created in thin single crystal plates of certain rare earth orthoferrites. Moreover, these domains may be moved freely about in two dimensions. Since this first publication a considerable amount of work has been carried out at Bell Telephone Laboratories and elsewhere on the physics and technology of magnetic bubbles, and on a range of devices using these. By early 1972 nearly two hundred had been published which show that the understanding of magnetic bubbles and their manipulations has reached an advanced stage but that commercial exploitation depends on economic production of improved materials.

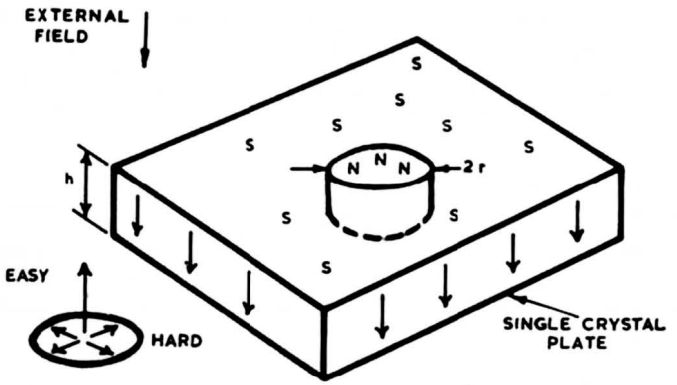

Fig. 11. Geometry of cylindrical magnetic domains.

The theory of stable cylindrical magnetic domains has been exhaustively treated in a paper by Thiele[64] which extends earlier theory. This shows that a cylindrical domain, such as shown in Figure 11, may be stable if the crystal plate of thickness h has uniaxial anisotropy with the easy axis normal to the plane of the plate. A further requirement also gives an optimum value for $h \approx$ bubble diameter. In general, a thin plate of uniaxial material will

show strip domains as illustrated in Figure 12(*a*). When a uniform magnetic field is applied normal to the plate, the domains magnetized in the field direction grow at the expense of the reverse domains. Eventually, a field is reached at which the closed strips shrink to cylinders; these are seen as dots in Figure 12(*b*). They are stable but decrease in size as the field is increased by a further amount (10% of the $4\pi M_s$ for orthoferrites) at which point they suddenly collapse leaving the plate uniformly magnetized in the field direction. These domains are readily observed by the Faraday effect as in Figure 12; polarized light is beamed through the plate and the oppositely magnetized domains are viewed through a crossed polarizer above the plate.

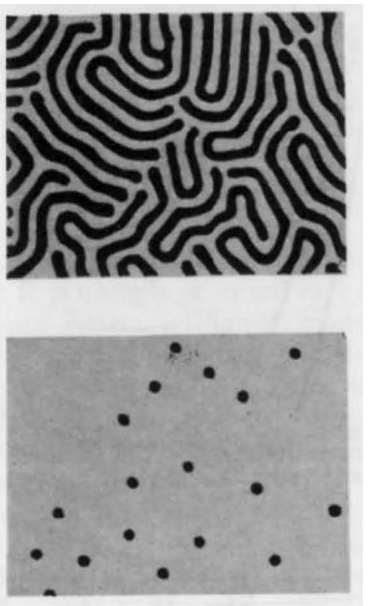

Fig. 12. (b) *When uniformly biased at 42 Oe external field the strip domains of* (a) *become cylinders* $1{\cdot}8 \times 10^{-3}$ *in dia.* (*Reference 65, Fig. 2.*)

The simplified theory of Thiele is given in a later paper by Bobeck.[65] This shows that cylindrical domains in a

plate of uniaxial magnetic material are stable under the action of three opposing forces. The forces acting on each domain from the uniform applied field and from the domain-wall energies both act to contract the domain. These are counteracted by the magnetostatic energy which acts to expand the domain to reduce the energy. These forces are in stable equilibrium under certain well-defined conditions which depend on the domain-wall energy σ_w(erg. cm^{-2}) and saturation magnetization M_s. This equilibrium region is shown in Figure 13; for high bias fields there is radial instability and the domains collapse, while for low bias fields the domains become elliptically unstable and form the characteristic strip domains. The bias field H_B to maintain domains at optimum plate thickness is $H_B \sim \dfrac{4\pi M_s}{3}$.

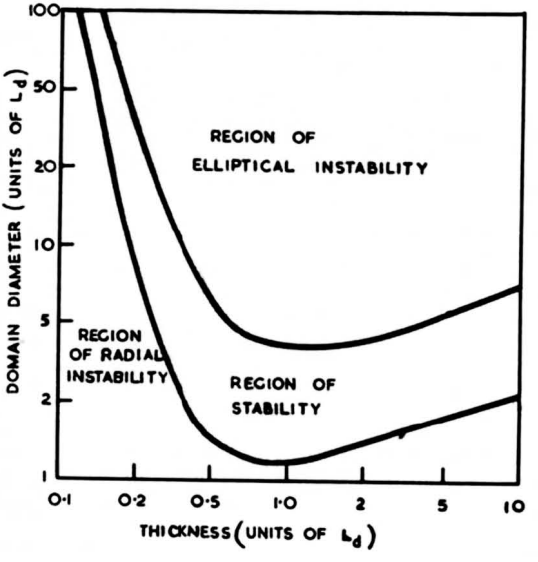

Fig. 13. Stability of cylindrical domains as a function of diameter and thickness (normalised to units of $L_d = \sigma\omega/4M_s^2$) with bias field as a parameter.

A further static stability requirement[66] is that the cylindrical domain shall not be self-nucleating. This condition

is met provided the sum of the bias and demagnetizing fields is less than the nucleation field H_N, viz.

$$H_N > 4\pi M_s + H_B.$$

We have seen above that H_B is somewhat less than $4\pi M_s$, thus to a first approximation $H_N > 4\pi M_s$. In a perfect crystal with no defects $H_N = H_A$ (the anisotropy field). Thus to support stable cylindrical domains the single crystal ferrite must have $H_A > 4\pi M_s$. A further requirement is that the domain wall-mobility shall be high to allow rapid movement of the domains from one position to another.

A wide range of magnetic materials, which meet these various requirements, are discussed in Reference 66. It was concluded that the uniaxial hexaferrites and the rare earth orthoferrites were the most promising available materials to give domains of less than 10 μm diameter.

Much of this earlier and subsequent work has been carried out on the rare earth orthoferrites. These are antiferromagnetics of orthorhombic structure having composition $RFeO_3$, where R is a single or mixed rare earth ion. The anti-parallel spin system is slightly canted out of the c-plane to give a small net magnetic moment in the c-direction ($4\pi M_s \sim 100$ Gs (0·01 T) at room temperature) up to the Néel point (400°C). An exception to this rule is $SmFeO_3$, which has its net moment along the a-axis at room temperature. Anisotropy fields H_A are high, being between 2×10^3 and 5×10^5 Oe dependent on composition, giving domain diameters from ~100 μm ($YbFeO_3$) down to ~40 μm for $TbFeO_3$. Plate thicknesses L_D for these are slightly less than the diameters of the domains. Further reduction of the domain diameter is achieved by lowering σ_w by means of a substitution of samarium for terbium. This reduces anisotropy by virtue of the fact that the easy axis of magnetization of $SmFeO_3$ is along the a-axis rather than the c-axis as for the $TbFeO_3$. The composition $Sm_{0.55}Tb_{0.45}FeO_3$ has $L_D = 10$ μm and domain diameter of ~18 μm.[65]

Recent work at Bell Telephone Laboratories has shown that some rare earth iron garnets grown from flux melt have a cubic distortion related to the {211} growth faces.[67] This distortion causes a uniaxial anisotropy H_A in a {111} direction, either normal to, or in the plane of a {211} facet, dependent on composition. The H_A is greater than the $4\pi M_s$ of the crystal, hence bubble domains may exist under the conditions described above. By selecting compositions with low magnetostriction, such as $Gd_{2.34}Tb_{0.66}Fe_5O_{12}$, domains of 6 μm diameter and high mobility have been observed. Other workers have produced mobile domains in epitaxial garnet films grown by vapour deposition on non-magnetic garnet substrates.[68] This work adds another class of potentially useful materials to those discussed above.[67]

Experimental work on bubble domain devices requires high perfection in the thin plates of the ferrite crystals, as defects such as pores and cracks, even of microscopic size, will pin the domain walls. Strains in the plates due to uneven growth, or machining and polishing, also inhibit free movement of the domains. These defects may be reduced in the orthoferrites by a very high temperature anneal under carefully controlled conditions[69] to give coercivities as low as 0·5 Oe. These crystal plates have been used by the Bell Telephone Laboratory workers to fabricate a range of bubble devices for digital systems.[65, 70, 71]

Present applications appear to be for memories, logic circuits, and shift registers. The highly localized magnetic fields required to propagate and create domains were produced in the earlier circuits by small conductor loops printed on the plate surface.[65] These were arranged in orthogonal patterns for two dimensional propagation, or linear patterns for shift registers. Output loops detected the presence or absence of a bubble by change of flux when it was removed or collapsed. Alternative non-destructive read-out made use of the Faraday effect with polarized light which excited a photo-conductive diode. Hall effect and magnetoresistive devices may also be

deposited on the crystal to provide non-destructive read-out. Other more recent geometries make use of patterns of low coercivity "Permalloy" which overlay the conductor patterns. These interact with the field above the surface due to the bubble domains and trap the bubbles. By magnetizing the magnetic overlay with an externally applied magnetic field the bubbles may be propagated along paths defined by the magnetic overlay. A simple arrangement known as "T-BAR" uses T- and I-shaped areas of "Permalloy" as shown in Figure 14. Application of a continuously rotating magnetic field moves the bubble domains one complete step for each period of rotation.

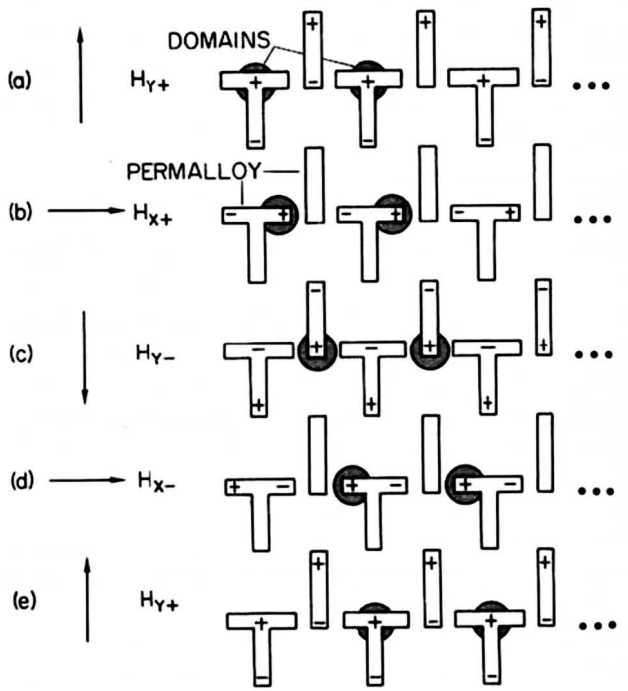

Fig. 14. Bubble domain propagation using the T-BAR permalloy pattern in a rotating magnetic field. As the field rotates free poles appear on the T's and bar causing the bubbles to move. (*After Reference* 70.)

Packing densities of experimental circuits are 10^4 bits/in^2

for conductor patterns and 10^6 bits/in^2 for the T-BAR patterns. Wall velocity for the $Sm_{0.55}Tb_{0.45}FeO_3$ crystals is the order of 5×10^3 cm.sec^{-1} limiting cycle times to 5 μs. Bit rates in excess of 10^5 bit.sec^{-1} and packing densities up to 10^6 bits/in are expected from the uniaxial garnet materials having bubble domain diameters of $\sim$8 μm.

7. Ferrites for Microwave Applications

Ferrites were in general use for inductor and transformer cores by the early-1950s when attention was turned to the unique properties of these materials at microwave frequencies (i.e. between 1000 MHz and the infra-red). These properties were found of use in a new class of microwave components which have been continually expanded and improved up to the present time. These components have required an increasingly wide range of high quality ferrites which have been developed in parallel. Compositions in all three structural classes of ferrite have been optimized for use at microwave frequencies. These are often described in the literature as "microwave" ferrites, but are, in fact, closely related to those used at lower frequencies.

As these ferrites are so closely linked with microwave component development, the principles of operation of microwave components will be discussed before considering those ferrite materials which are currently in use and under development.

7.1. FERRIMAGNETIC RESONANCE

It is found that as frequency is increased up to microwave frequencies the ferrite permeability μ' decreases rapidly to less than 1, as shown in Figure 15. The curve, and its associated magnetic loss μ'', shows two relaxation frequencies, one at around 50 MHz due to magnetic domain-wall resonances and another at a higher frequency of 1500 MHz. It is this latter relaxation or resonant frequency of the ferrite material which is exploited in the specialized applications of ferrites at microwave frequencies.

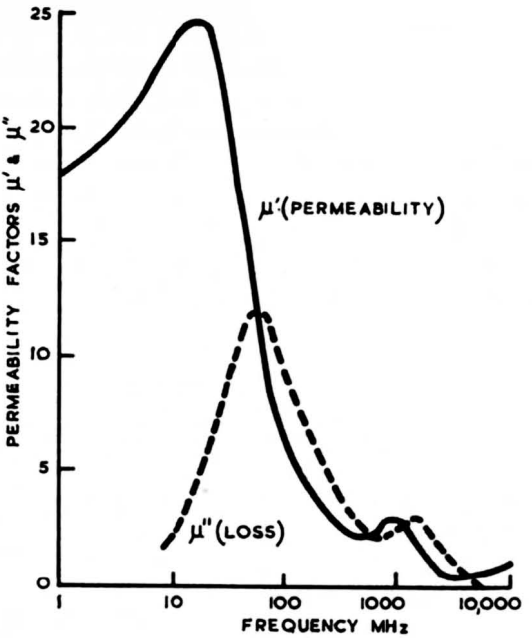

Fig. 15. Complex permeability of polycrystalline ferrite showing ferrimagnetic resonance at 1500 MHz.

Landau and Lifshitz showed in 1935 that the orbital electrons of the magnetic ions of a magnetic material will precess when disturbed, due to their having angular momentum about their spin axis. The frequency of precession is proportional to the magnetic field H in which the electron is situated, with a constant of proportionality γ close to 2·8 MHz/Oe. This resonance due to precession of the electrons is similar to the precession of a gyroscope, and it is frequently termed *gyromagnetic resonance*. It is observed both in ferromagnetic materials and in ferrites, being more exactly called ferromagnetic resonance in the one and ferrimagnetic resonance in the other. In moderate magnetic fields the resonance will occur at microwave frequencies, but is of small amplitude in ferromagnetics due to the small skin depth arising from their conducting properties. However, in the case of ferrites with high resistivity the resonance is of large magnitude as e.m. waves will penetrate these materials. This indicates that

the prime requirement of a ferrite to be used at microwave frequencies is that it should have low dielectric loss, tan δ. Most microwave ferrites are prepared in such a way as to have tan $\delta < 0{\cdot}001$, whilst some have tan δ as low as 0·0001. The ferrimagnetic resonance seen in Figure 15 at 1500 MHz is somewhat diffuse, as resonance in the unmagnetized ferrite is caused by random internal fields due to spontaneous magnetization and magnetocrystalline anisotropy which both vary from point-to-point.

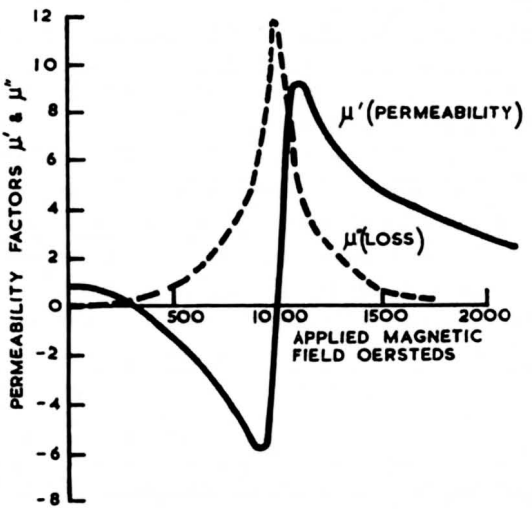

Fig. 16. Gyromagnetic resonance of ferrite sphere at frequency of 2800 MHz.

If a strong external field is applied to saturate the ferrite, then the spins are aligned and a discrete resonance is observed. However, due to the internal demagnetizing field caused by free poles on the ferrite surface, the internal field is not uniform unless the ferrite is ellipsoidal in shape. If, for example, the ferrite is spherical, then μ' and μ'' have the form shown in Figure 16. This resonance is dependent on the shape of the sample, and it is that normally observed in ferrites. It is named after Kittel, who first derived the equations relating resonant frequency to sample shape. The theory and early references are dealt with at length in References 72 and 73. Further extensions

of this theory relate resonant frequency to shape anisotropy for single crystals and aligned ferrites having magnetocrystalline anisotropy.[74] Although mainly of theoretical interest it should be noted that the observed Kittel resonance does not in general occur at ferrimagnetic resonance. This point is discussed at length in Reference 73.

The magnetic loss factor μ'' is found to vary with compositions and preparative conditions (microstructure) of the ferrite; it is therefore an important parameter in assessing microwave ferrites. It has been common practice to describe magnetic loss in terms of the linewidth ΔH measured as the -3dB width of the μ''vH characteristic of a sphere at resonance. However, it is now recognized[75] that this parameter does not express the loss away from Kittel resonance where the effective linewidth ω of a polycrystalline ferrite may be only 1/20th of the ΔH at resonance, as shown in Figure 17. The explanation of this[76] lies in the existence of spin waves in ferrite materials.

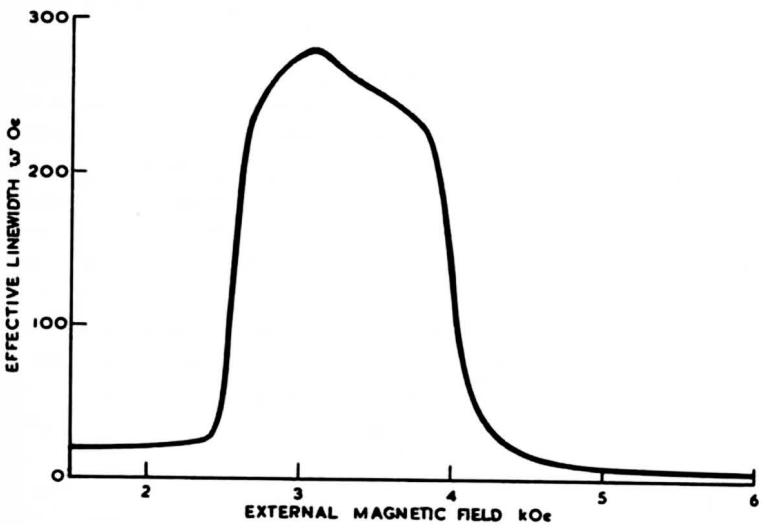

Fig. 17. Variation of effective linewidth W with external magnetic field measured on low porosity nickel ferrite ($NiMn_{0.05}Fe_{1.95}O_4$) *spheres at 9·005 GHz. (After Reference 75.)*

Spin waves in ferrites were first discussed by Suhl[77] who obtained their dispersion relation in a magnetized ferrite. They have since been investigated extensively by physicists to explain the mechanisms by which magnetic energy is coupled to the lattice to be dissipated as heat; spin waves also are responsible for the non-linearities which are found when the spin precession is driven by high microwave magnetic fields. A description of spin waves is outside the scope of this review, but the basic theory as applied to ferrites is outlined in Reference 72 and treated more exactly in References 78 and 79. The subject will be taken up again later in discussing certain applications of ferrites which are dependent on the special properties of spin waves.

As well as the requirement of low dielectric and magnetic loss, microwave ferrites are often required to have specific values or limitations of saturation flux density $4\pi M_s$. This arises because any region of unsaturated ferrite will have internal fields due to porosity and magnetocrystalline anisotropy H_A, of up to a maximum of $(4\pi M_s+H_A)$. Resonance absorption of microwave energy due to these fields will occur to a limiting frequency of $\gamma(4\pi M_s + H_A)$. Thus, if this "low field" loss is to be avoided, the ferrite should not be used below a frequency of $\gamma(4\pi M_s + H_A)$. Hence, for any required operating frequency there is a maximum value of $4\pi M_s$, H_A being negligible in soft ferrites. The other properties such as temperature stability of $4\pi M_s$ and non-linearity are also important for optimum device design, and often determine the composition chosen for a particular application.

7.2. MICROWAVE DEVICE APPLICATIONS

The gyromagnetic resonance in magnetized ferrite is excited by a circularly polarized r.f. magnetic field rotating in a plane normal to the direction of magnetization in the same sense as the spin dipole precession. It is not excited by a pure circularly polarized contra-rotating field. Thus, since the sense of rotation of the circularly

polarized components of a travelling electromagnetic wave is reversed with reversal of wave direction, a magnetized ferrite will interact differently according to both the polarization and direction of the wave. This non-reciprocal behaviour of the ferrite can be used in a wide range of microwave devices having unique transmission properties which may be constructed in waveguide, coaxial, or stripline geometry.

These devices divide into two main categories, (i) those showing linear transmission properties, and (ii) those with non-linear responses. The first is the more important, accounting for the majority of production devices, whereas the second category now consists only of limiters for protection of sensitive receivers against damage from high power inputs.[78, 80]

The earliest microwave ferrite devices made use of the non-reciprocal resonance absorption of ferrite biassed to Kittel resonance by the field from a permanent magnet. By use of this effect a section of waveguide containing the ferrite will pass microwave energy flowing in a forward direction, but will absorb substantially all energy at the same frequency flowing in the reverse direction. This device is a *resonance isolator.*

The precession of spin dipoles in the magnetized ferrite at frequencies below resonance was also found to cause rotation of the plane of polarization of microwave energy propagating in the direction of magnetization. This is microwave Faraday rotation, by analogy with the same effect observed with visible radiation. Non-reciprocal phase shift could also be obtained by inserting transversely magnetized ferrite plates in rectangular waveguide. A new device, the four-port circulator, could then be realized by combining two 3 dB couplers with an interposed non-reciprocal phase shifter. This device has low loss from port 1 to 2, 2 to 3, 3 to 4 and 4 to 1, but high isolation in the reverse direction (1 to 4, 4 to 3, etc.). It is employed for example to separate the transmit–receive signals at the

common aerial of a radar system, and to combine or separate channels in microwave telecommunication systems. These various devices were in wide use by the early-1960s, and are described fully in Reference 72.

The junction circulator, another form of circulator which appeared at this time, has been extensively studied during the last decade. This has only three ports, but is of simple construction as couplers are not needed to obtain circulation. The current theories of operation of the waveguide, stripline and lumped impedance forms of this device are summarized in Reference 81. Operation has been seen as low as 30 MHz, whilst waveguide circulators have been made for use up to 100 GHz. Its versatility has resulted in its being the most widely used microwave ferrite device at the present time. Octave bandwidths are readily achieved or extremely low forward loss ($<0{\cdot}1$ dB) combined with high isolation (>30 dB) over narrower bands ($\sim 10\%$).

Addition of a matched load to one port turns the circulator into an isolator (the so-called isocirculator), and by building a compact load into the circulator itself the isocirculator may be made extremely small. Figure 18 shows some typical junction circulators for use between 1 and 12 GHz. The development of improved circulators has required parallel improvements of ferrite materials, particularly to achieve low loss, good temperature stability and operation at high microwave power levels.

Similar material improvements have been made for the ferrites used in electronically controllable phase shifters which are finding application in steering radar beams from fixed multiaperture antennas. These phase shifters[82] have been developed in geometries for which separate sections can be switched between two levels of phase shift by control pulses. Thus, a four-section phase shifter has sections which can be independently set at 0 or $\pi/8$, 0 or $\pi/4$, 0 or $\pi/2$, and 0 or π, giving the possibility of any total phase shift from 0 to 2π in $\pi/8$ steps. This form of

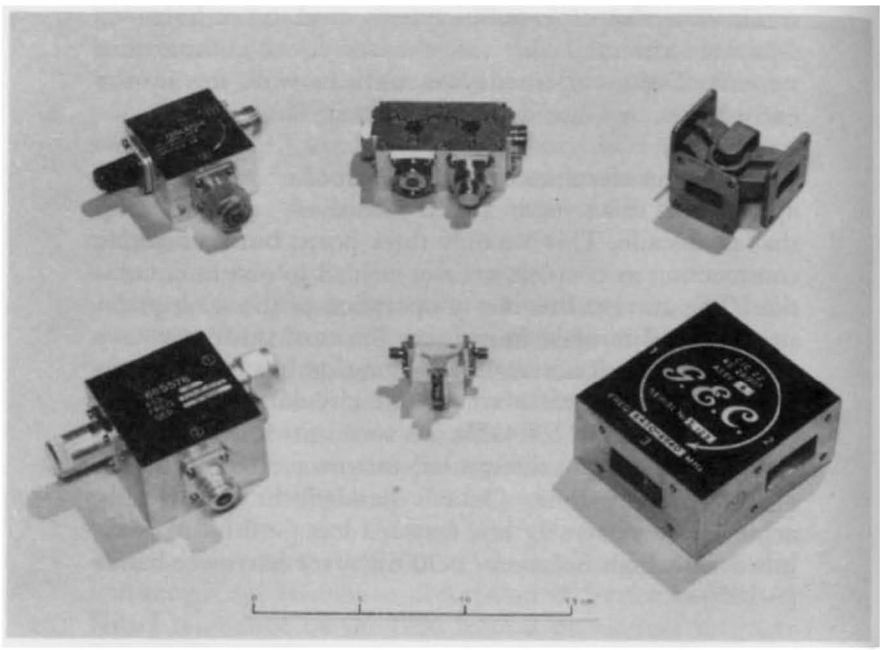

Fig. 18. Typical circulators and isocirculators. Top row L to R, 4 GHz stripline isocirculator, 7·5 GHz 4-port stripline circulator, 9–10 GHz waveguide circulator; bottom row L to R, 2 GHz stripline isocirculator, 6 GHz microstripline circulator and 6 GHz waveguide circulator.

operation has the advantage of giving computerized digital control of the radar-beam direction. Such devices are named in the literature as *latching phase shifters*. A recent development[83] has shown that by loading the ferrite in a waveguide phase shifter with a high permittivity dielectric ($\varepsilon > 30$) the performance and size may be considerably improved. This work also suggests that the cost may be reduced, an important advantage as a single aerial uses at least 2500 phase shifters.

A number of new devices developed during the period 1968–71 are already being designed into present generation microwave systems. These are the microstrip circulator[84] designed for use in microwave integrated circuits, the printed circuit circulator[85] which although less than 1 cm in diameter gives broadband circulation as low as 1 GHz, and the edge mode isolators having bandwidths in excess of an octave. Full details of the latter have yet to be published, but References 86 and 87 give some indication of the principle of operation.

The devices so far described use polycrystalline ferrites. A further device is the electronically tuned filter which uses two or three small polished spheres of single crystal yttrium iron gallium garnet in a filter network.[88] The spheres show high-Q Kittel resonance in a uniform magnetic field yielding a band-pass response at this frequency. The centre frequency of the filter may be readily varied over an octave by sweeping the magnetizing field derived from a compact electromagnet. In a more basic form the yttrium iron garnet spheres may be used to control or sweep the frequency of solid state oscillators.[89]

7.3. CURRENT DEVELOPMENT OF MICROWAVE FERRITE MATERIALS

At frequencies up to 30 GHz the "soft" spinels and garnets are employed in the many devices described in Section 7.2. Above 30 GHz the "hard" hexaferrites are often used in resonance isolators. The polycrystalline hexaferrite is aligned during manufacture, as described in Section 4 on permanent magnets, to provide an internal anisotropy field of up to 17 kOe to obtain Kittel resonance without the need for high applied fields from an external magnet.

Spinels and garnets are largely complementary to each

other in device applications. The spinels are employed where moderate to high saturation magnetizations are usable, i.e. at intermediate microwave frequencies and above. The garnets are chosen for their lower saturation magnetization values, which are required at low microwave frequencies to avoid "low field" loss in the unsaturated ferrite. This is particularly important in circulators and latching phase shifters, where unsaturated regions are almost always present in the ferrite due to the low operating fields and non-ellipsoidal geometries.

Spinels were the first ferrites to be used at microwave frequencies. Many of these, with the major exception of the ferrous ferrites which show high dielectric losses, have been prepared with suitably low dielectric loss for microwave use. However, at the present time, only the nickel and magnesium ferrites with small additions of zinc, manganese, cobalt or copper to improve dielectric loss, or modify saturation magnetization, find frequent use. The most usual means of reducing $4\pi M_s$ is to replace Fe^{3+} by non-magnetic aluminium. The Curie temperature at which the ferrite loses its ferrimagnetic properties is reduced in proportion to this substitution, thus worsening the stability of saturation magnetization with temperature.

An unusual spinel-structured ferrite of microwave interest is lithium ferrite in which the divalent ions of normal spinels have been replaced by equal proportions of monovalent lithium and trivalent iron to give the molecular composition $(Li^{1+}_{0.5}Fe^{3+}_{0.5})Fe^{3+}_{2}O_4$. This has high saturation magnetization (3600 Gs) and low linewidth ΔH. However, the polycrystalline material is difficult to sinter to high density without loss of lithium, and current work[90] is directed towards obtaining a ceramic lithium ferrite with the properties expected from single crystals.

The properties of spinel-structured ferrites are given in detail in Reference 91, which has gathered together much of the published properties of microwave ferrites. The commonly used magnesium ferrites, however, have received little attention in the literature. These have high

Table 7. Typical microwave properties of some spinel-structured ferrites

COMPOSITION	SATURATION MAGNETIZATION $4\pi M_s$ Gs	DIELECTRIC CONSTANT	DIELECTRIC LOSS tan δ	LINEWIDTH Oe	CURIE TEMPERATURE °C	TEMP.* STABILITY OF $4\pi M_s$ % per °C
Magnesium–manganese ferrite	2300	13·0	0·0003	300	310	0·25
Magnesium–manganese aluminium ferrite	1200	12·0	0·0005	120	150	0·7
Nickel ferrite	3200	13·5	0·001	350	590	0·11
Nickel–aluminium ferrite	2250	11·0	0·001	500	550	0·13
Nickel-zinc ferrite	5000	12·5	0·001	130	370	0·2

*From −20 to +80°C. (*Note:* 1 Oe = 80 Am^{-1}; 1 Gs = 10^{-4}T.)

conductivity loss when stoichiometric, but workers in the U.S. showed more than a decade ago that if prepared with an excess of magnesium, and a low level of added manganese, then a combination of low dielectric and magnetic losses could be obtained.[92] These magnesium–manganese ferrites have poorer temperature stability than the nickel ferrites with aluminium substitution giving the same saturation magnetization. The nickel ferrites have the disadvantages of higher losses. These properties are briefly compared in Table 7.

Spinel materials produced by conventional ceramic processing techniques from mixed oxides normally have microstructures with average grain size of 10 to 20 μm. It has been shown[93] that if the grain size, or intragranular pore spacing, can be made comparable to the wavelength of the longer wavelength spin waves, then these are scattered and the critical r.f., field strength, at which the ferrite shows non-linear loss, is raised. This technique can be used to increase the peak power-handling capability of existing devices, without change of geometry, as fine-grained ferrites have closely similar properties to the coarser-grained material of the same composition. A slightly higher magnetic loss at low powers is the only penalty of using the fine-grained ferrites. This arises since magnetic loss at low power levels is also caused by scattering of spin waves by imperfections as previously discussed.

Table 8. Influence of composition and grain size on loss and power-handling capability of X-band junction circulator

FERRITE	GRAIN SIZE μm	SATURATION MAGNETIZATION $4\pi M_s$ Gs	LOSS AT LOW POWER dB	PEAK POWER* LEVEL kW
Magnesium–manganese	10	2300	0·10	1·5
Magnesium–manganese	4	2300	0·11	6·0
Nickel aluminium	10	2250	0·3	60

*Power above which insertion loss increases rapidly.

Experimental work has shown that the critical field of nickel ferrites is higher than one would expect from a

study of the magnesium ferrites, but as in the previous example the magnetic loss is also found to be higher. These effects are demonstrated by the performance of an *X*-band junction circulator using these ferrites given in Table 8.

In 1956, a distinct crystalline phase in the rare-earth iron oxide system was identified as having the garnet structure with molecular composition $R_3Fe_5O_{12}$, where R is a rare-earth ion (or combination of rare-earth ions), usually the non-magnetic yttrium ion Y^{3+} (Table 1). It is of interest to note that unlike the spinels, where both divalent and trivalent ions are present, ideally only trivalent metal ions are in the pure garnets. Electron transfer is precluded and the garnets are therefore characterized by very high resistivity and thus low dielectric loss. This, combined with relatively low anisotropy, makes them particularly suitable for microwave applications. It is also easy to prepare moderate sized single crystals of the rare-earth garnets, and the properties of these have been accurately determined and reported in the literature.[91] The single crystal yttrium–iron garnet (YIG) and the lower saturation yttrium–iron–aluminium garnets (YIAlG) are now used in electronically tunable filters and oscillators, but there are as yet no other commercial applications of importance. Polycrystalline garnets, extensively used in circulators and phase shifters, are of greater engineering importance.

At u.h.f., low-saturation magnetization garnets must be selected to avoid low field loss. This may be done, as with spinels, by replacing iron with aluminium (or gallium); thus, the room-temperature $4\pi M_s$ of $Y_3Fe_5O_{12}$ reduces monotonically with this substitution from 1760 Gs to zero for the composition close to $Y_3Al_{1\cdot8}Fe_{3\cdot2}O_{12}$. This depression of the Curie temperature leads, as in the spinels, to poor temperature stability for the low $-4\pi M_s$ garnets. However, the substitution of gadolinium for yttrium also has the effect of reducing $4\pi M_s$; but, owing to the magnetic interaction of the Gd^{3+} ion, the Curie temperature of 280°C for YIG is unchanged and a compensation tem-

perature at which $4\pi M_s$ falls to zero appears at low temperatures. This leads to an improvement of the $4\pi M_s$ v. temperature characteristic over a practical working range.[94, 95]

The lowest magnetic and dielectric losses can only be achieved in rare-earth garnets by careful control of composition.[96] Excess iron causes uncontrolled grain growth and high losses. Iron-deficient garnets are difficult to sinter, unless undesirable impurities are introduced, and they show higher losses than materials with compositions stoichiometric to 0·1%.

The magnetic loss and resonance linewidth of yttrium-gadolinium garnets increase with increasing gadolinium content, e.g. the linewidth of temperature-stable crystalline $Y_{1\cdot8}Gd_{1\cdot2}Fe_5O_{12}$ is 150 Oe compared with 40 Oe for YIG. Reduction of $4\pi M_s$ can be achieved, as previously discussed, by substitution of aluminium for iron with little effect on linewidth at room temperature. This suggests a compromise solution[94] for obtaining the best temperature stability with lowest linewidth (or magnetic loss) in compositions of the type $Y_{3-x}Gd_xFe_{5-y}Al_yO_{12}$. These give optimum compositions as indicated in Reference 94, such as $Y_{2\cdot2}Gd_{0\cdot8}Fe_{4\cdot5}Al_{0\cdot5}O_{12}$.

The general study of rare-earth garnets has shown that certain rare-earth ions act as scattering centres for spin waves,[78] thus causing high spin wave linewidths. Some of these ions, notably holmium, terbium and dysprosium cause this effect at low concentrations of less than 1% in YIG. It is therefore essential to hold these rare-earths to low impurity levels in YIG if narrow linewidth is required as for filter applications, or if low magnetic loss is wanted for devices such as circulators. Large spin wave linewidth also leads to high critical field which is desirable in high power devices. Thus, garnets for these applications often have these rare-earths introduced at carefully controlled levels; the disadvantage is a significant increase in insertion loss due to the high magnetic loss of the added rare-earths.

In 1963, workers at the Bell Telephone Laboratories in the U.S.A., who were engaged on an extensive exploration of garnet-structured ferrites, discovered a range of garnet compositions which are ferrimagnetic at room temperature, but do not contain rare-earth ions.[97] These are calcium–vanadium–iron garnets in which bismuth is substituted for calcium, with a change in vanadium content to maintain valency balance according to the general composition $Bi^{3+}_{3-2x}Ca^{2+}_{2x}Fe^{3+}_{5-x}V^{5+}_{x}O_{12}$. Preparative techniques suitable for these garnets are found to be similar to those for other ferrites. The firing conditions are, however, critical. Relatively low temperatures between 1100 and 1200°C are used, dependent on composition. Firing in oxygen as opposed to air improves sintering and reduces losses.[98]

Curie temperature and temperature stability of magnetization are high for the relatively low values of $4\pi M_s$ (200 to 750 Gs dependent on composition) compared with rare-earth garnets; dielectric loss can be low, as can linewidth and magnetic loss. These "yttria-free" garnets are also characterized by fine-grain structure, and have high values of critical field. Furthermore, the cost of raw materials is low compared with garnets using the expensive rare-earth oxides. This combination of attributes makes them attractive for use in very high power latching phase shifters and in u.h.f. circulators. They are brittle, however, and require more care in machining than the conventional garnets.

Two developments which are significant for device applications concern the use of additives. It has been found that the addition of indium reduces the anisotropy of YCaVIG substantially to zero. Since the increase of resonance linewidth is due to a combination of porosity and anisotropy it has been found[99] that very dense garnets of this composition may have linewidths as low as 8 Oe at room temperature. Magnetostriction in spinels and garnets reduces the remanent magnetization which is a key parameter for latching phase-shifters. Dionne[100] has shown

that manganese doping at levels of only 1% reduces magnetostriction and increases remanence.

The high anisotropy of the hexaferrites is used to obtain Kittel resonance in mm wave devices at relatively low external applied fields. Many of the hexaferrite compositions described in Reference 101 have been prepared as aligned polycrystalline ceramics by pressing in a magnetic field prior to sintering, as discussed in the Section 4 on hexaferrites (unaligned hexaferrites have unacceptably high linewidths and magnetic loss).

Early work was done with barium hexaferrite, which was prepared with low dielectric loss and linewidth of around 1150 Oe. The anisotropy field is 17 *k*Oe, and since the internal field cannot be reduced by an external applied field the lowest Kittel resonance is at 48 GHz (6 mm wavelength). For lower frequencies, various substituted hexaferrites with lower anisotropies have been examined.[102] A promising material is nickel–cobalt–*W* of composition $BaNi_{2-x}Co_xFe_{16}O_{27}$ where *W* designates the $[BaFe_{16}O_{27}]^{4-}$ ion. This is a solid solution of Co_2W in Ni_2W; the uniaxial anisotropy of the latter is progressively reduced to zero as the cobalt content is increased. It has been found possible to prepare these compositions with anisotropy field as low as 3000; this has been used in an X-band isolator operating with an external applied field of only 200 Oe.[92] At the present time there is little interest in hexaferrites for mm wave applications, as the spinels can be used in phase shifters and junction circulators using conventional magnet systems for frequencies of current interest up to 40 GHz. The use of frequencies up to 110 GHz for telecommunication systems operating in circular waveguide will renew interest in the hexaferrites.

8. Magneto–elastic Waves in Yttrium–Iron Garnet

A progressive wave motion may be excited in a single crystal magnetic material which is dependent on the same properties of the precessing magnetic dipoles (electrons) as is the non-reciprocal behaviour of ferrites at microwave frequencies, discussed in Section 7. These progressive waves are known as *spin waves*. They arise from exchange coupling between the spins, whereby any disturbance of one spin causing it to precess (at a microwave frequency) is coupled to adjacent spins and so on through the crystal, thus propagating energy in all directions away from the point of disturbance. The propagation constant for spin waves is very complex compared with electromagnetic or acoustic waves, being dependent on direction relative to the applied magnetic field (which aligns the spins), on the magnitude of the field, and on the demagnetizing factors.[103] In the simple case of spin waves with wavelengths short compared with sample dimensions propagating in the direction of the local field (H) then

$$\omega = \gamma H + \gamma D k^2$$

where D is the exchange constant (equal to 5×10^{-9} Oe cm^2 for yttrium–iron garnet) and k is the wave number. (Ferrimagnetic resonance is the special case of this equation for $k = 0$.)

This relation is shown in Figure 19(a), which includes the deviation occurring when the spin wavelength becomes comparable with sample size (the so-called magnetostatic wave region). The changeover from spin to magnetostatic waves is at a wave number $k_0 \approx 10^4$ cm^{-1}. In Figure 19(b), this dispersion curve is redrawn together with that for a transverse elastic wave which may also propagate in the garnet crystal. The so-called magneto-elastic wave is that which exists in the region C where both elastic and spin waves have the same phase velocities.

In this region, energy may be transferred from one wave to the other.

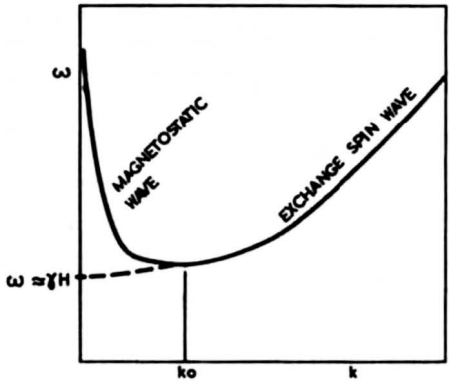

(a)

Fig. 19. (a) *Dispersion curves for spin waves: neglecting dipolar effects (dashed curve), including dipolar effects (solid curve).*

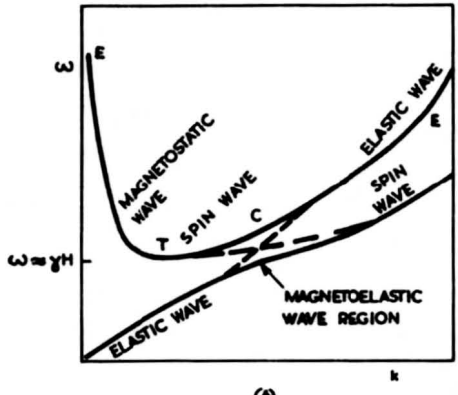

(b)

Fig. 19. (b) *Dispersion curves for spin and elastic waves: without magneto-elastic coupling (dashed curves), with magneto-elastic coupling (solid curves).*

If we now consider wave propagation along the axis of a YIG rod, axially magnetized by a uniform external magnetic field, we find that this is determined by the internal field directed along the axis.[104] This is least at the ends of the rod and maximum at the centre, as shown in Figure 20(*a*). If wave motion is now excited in

the YIG rod by a pulsed electromagnetic wave of frequency ω, we observe two important forms of response which depend on the magnitude of the applied field.[105] These are shown schematically in Figures 20(*b*) and (*c*). In the first, a magnetostatic wave is excited at the endface due to the dipole moment at the discontinuity caused by the YIG-air interface. This propagates along the axis of the rod to be reflected at the point T at which ferrimagnetic resonance occurs, i.e. where $\gamma H_{INT} = \omega$. The reflected wave will then give an echo when it reaches the endface of the rod, the delay time being dependent on the applied field which determines the position of T.

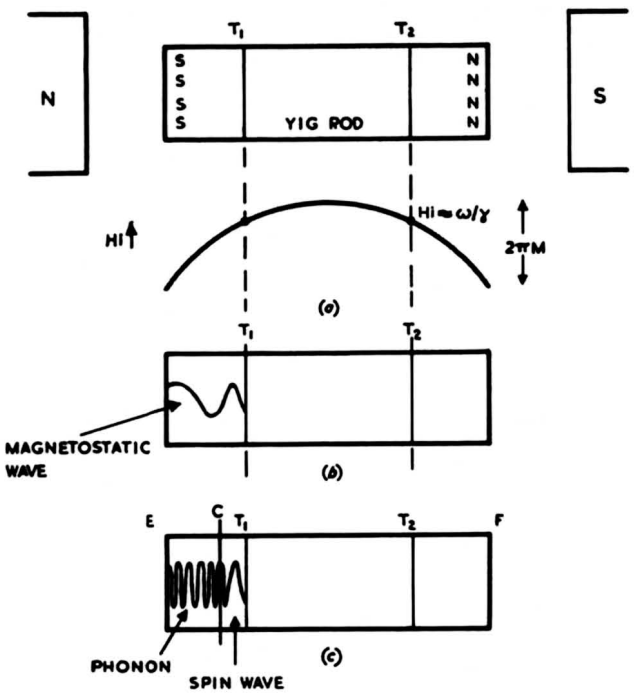

Fig. 20. (a) *Axially magnetized YIG rod showing turning points* T_1 and T_2.

(b) *Sketch of magnetostatic wave in rod and variation of axial field Hi.*

(c) *Separation of magneto-elastic wave into spin-wave and elastic-wave components.*

Figure 20(*c*) shows a second condition for an even higher applied field. The magnetostatic wave generated at the endface *E* travels to point *T*, where it largely converts to a spin wave which travels back towards *E*. However, at a point *C* corresponding to the crossover point in Figure 19(*b*), the spin wave converts to an elastic wave which is then reflected at *E* to be reconverted to a spin wave at *C* and then a magnetostatic wave at the turning point *T*. This returns to the endface *E* where it is detected as a pulse of electromagnetic energy. Delay times for a 1 GHz pulse are related to applied field in Figure 21 for a 1-cm YIG rod. Modes *A* and *B* are due to the magnetostatic wave, and Mode *C* is the magneto–elastic condition described above for which energy converts from spin to acoustic waves. The overlap of *B* and *C* results from only partial conversion of magnetostatic wave energy to spin waves. These curves show that large delays may be obtained, which are adjustable by the external applied field. The insertion loss is relatively low, being around 25 dB compared with 80 dB for bulk elastic waves.

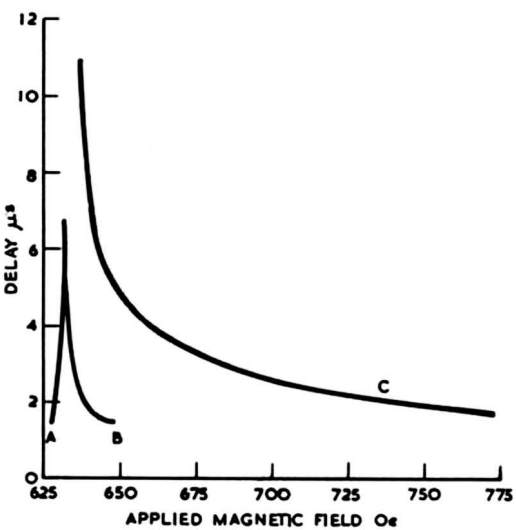

Fig. 21. Delay times for various modes at 1 GHz in an axially magnetized YIG rod. A = magnetostatic mode, B = reflected magnetostatic mode, C = magneto-elastic mode.

In addition to use of magneto–elastic YIG delay lines for radar signal processing,[106] the dispersive nature of the delay (1 μs/50 MHz) makes these devices useful in pulse compression radar. In these radars, the pulse is frequency modulated from the lowest to the highest frequency. The received pulse is then passed through a dispersive YIG delay line in which the lower frequencies are delayed more than the higher frequencies according to Figure 21 (for which $\omega \propto H$). Thus the leading edge of the pulse is delayed more than the trailing edge, and the pulse is compressed to give better target definition.

These delay lines have not as yet been used in operational radars, mainly due to the very severe requirements on the quality of the YIG crystal rods. Recent work on growth of epitaxial YIG of good quality gives promise of uniform internal field due to the large area-to-thickness ratio and improved performance.[107]

9. Magnetostrictive Ferrites

When a ferrite single crystal is magnetized it becomes deformed and the fractional change in length, or strain, λ is known as the *magnetostrictive constant.* This is usually measured at saturation, and is found to vary with crystal orientation. In the polycrystalline ferrite there is an average value λ_s which depends upon the crystal structure, i.e. cubic or hexagonal,[108]

Table 9. Saturation magnetostriction λ_s for typical ferrites at room temperature

FERRITE	λ_s
Fe_3O_4	$+40 \times 10^{-6}$
$MnFe_2O_4$	-5
$MgFe_2O_4$	-6
$Li_{0.5}Fe_{2.5}O_4$	-8
$Ni_{0.5}2n_{0.5}Fe_2O_4$	-11
$NiFe_2O_4$	-26
$CoFe_2O_4$	-110

The values of λ_s for a range of ferrites are given in Table 9. This shows the positive magnetostriction of ferrous ferrite (Fe_3O_4), which may be used to balance the negative magnetostriction of the other spinels by incorporating the Fe_3O_4 in solid solution to obtain increased permeability or square loop characteristics. Of particular importance is the high magnetostriction of cobalt ferrite of -110×10^{-6}, which compares with values of -50×10^{-6} and -34×10^{-6} for cobalt and nickel metals respectively. As with piezoelectric ceramics. a useful criterion of use as an electromechanical transducer material is the electromechanical coupling factor k. This is defined as the square root of the ratio of mechanical to magnetic stored energies.

Values for both the conducting magnetics (nickel and cobalt) and the ferrites range up to $k \sim 0{\cdot}35$.

The magnetostrictive metals have relatively high tensile strengths when compared with the ferrite ceramics, for which the ultimate strength is only 200 $kg.cm^{-2}$; thus, the metals are of particular use for high power transducers where the strains might fracture ferrite materials. However, the conductivity of the metals requires lamination for high frequency applications as for transformers and inductors. The ferrites do not, and may be used at higher frequencies and in complex shapes which would be impractical for laminated metals. Other properties which must be controlled are the magnetic loss, and, for some applications, the temperature stability.

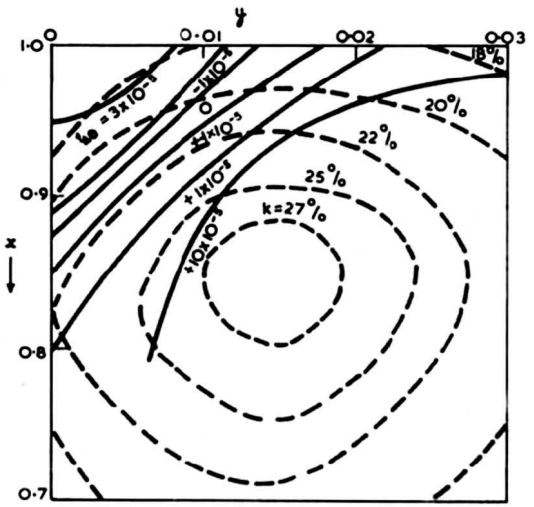

Fig. 22. Dependence of temperature coefficient of resonant frequency f_0 and electromechanical coupling factor k on composition of $[(NiO)_x(CuO)_{1-x}]_{1-y}[CoO]_yFe_2O_3$.

A number of magnetostrictive ferrites have been studied to optimize these various properties. Van der Burgt[109] discusses nickel–zinc–cobalt ferrites and concludes that these may be in many respects superior to piezomagnetic metals and alloys. They may be used in electromechanical

band pass filters. Japanese workers have extensively investigated the nickel–copper–cobalt ferrite system,[110] which combines high strength (up to 400 kg.cm^{-2}) with good electromechanical coupling, and low temperature coefficient of Young's modulus. This latter property controls the temperature stability of velocity of longitudinal acoustic waves and hence resonant frequency of a bar of the material. The curves of Figure 22 show that a composition $Ni_{0.93}Cu_{0.063}Co_{0.007}Fe_2O_4$ has good stability and electromechanical coupling, whilst

$$Ni_{0.84}Cu_{0.157}Co_{0.013}Fe_2O_4$$

has the highest coupling but poor stability.

Application of the magnetostrictive ferrites are mainly in electromechanical transducers for transmitting and receiving ultrasonic waves, and in magnetostrictive filters. For both these applications the ferrite must be partially magnetized by a bias field to avoid distortion. Otherwise a frequency doubling effect will occur, caused by the ferrite contracting for both the positive and negative half-cycles of the applied a.c. field. The bias may be obtained from d.c. in the winding or from a permanent magnet in the magnetic circuit of the transducer. The use of ferrite in electromechanical resonators for wave filters is of interest, since a prime requirement of these is very good temperature stability. Piezoelectric single crystals such as quartz may be cut with orientations to achieve this over a limited range, but the nickel–copper–cobalt ferrites shown in Figure 22 indicate that a magnetostrictive ceramic may give good stability of resonant frequency over a wide temperature range (+20 to +100°C). This application would, however, require careful control of fabrication of the ferrite to minimize aging effects as in the inductor core ferrites.

Appendix

MAGNETIC UNITS

The standard literature on ferrites still extensively uses the CGS system of units instead of the preferred MKS system. The table gives the more important magnetic units for both systems together with the conversion factors.

Conversion factors for changing from CGS to MKS magnetic units

QUANTITY	CGS UNIT	MKS UNIT	CONVERSION FACTOR FOR CGS TO MKS UNITS
Magnetic field H	Oersted	Ampere turns m^{-1}	$\times \frac{10^3}{4\pi}$
Magnetic flux ø	Maxwell	Weber	$\times 10^{-8}$
Flux density B	Gauss	Tesla	$\times 10^{-4}$
Magnetomotive force	Oersted cm	Ampere turns	$\times \frac{10}{4\pi}$
Intensity of magnetisation J	emu	Weber m^{-2}	$\times 4\pi.10^{-4}$
Magnetic moment M	emu	Weber m	$\times 4\pi.10^{-10}$
Pole strength m	emu	Weber	$\times 4\pi.10^{-8}$

References

1. M. M. Schieber, *Experimental Magnetochemistry, Nonmetallic Magnetic Materials*, North-Holland Publishing Company, Amsterdam, 1967, chap. 4.
2. L. G. van Uitert, "Dielectric properties of and conductivity in ferrites," *Proc. I.R.E.*, vol. 44 (1956), p. 1294.
3. J. Smit and H. P. J. Wijn, *Ferrites: Physical Properties of Ferrimagnetic Oxides in Relation to their Technical Applications*, Philips Technical Library, 1959. Distributed by Cleaver-Hume Press Ltd., London, chap. VIII, section 32.2.
4. L. Néel, "Magnetic properties of ferrites: ferrimagnetism and antiferrimagnetism", *Ann. Phys.*, vol. 3 (1948), pp. 137–198.
5. W. H. von Aulock, *Handbook of Microwave Ferrite Materials*, Academic Press, New York, 1965, chaps. 3–6.
6. J. Smit and H. P. J. Wijn, Ref. 3, chap. VIII, section 32.1, 1959.
7. D. J. Craik and R. S. Tebble, *Ferromagnetism and Ferromagnetic Domains*, North-Holland Publishing Company, Amsterdam, 1965, chap. 7.
8. D. Swallow and A. K. Jordan, "The fabrication of ferrites", *Proc. Brit. Ceram. Soc.*, vol. 2 (December 1964), p. 1.
9. C. S. Brown, "The effect of ceramic technology on the properties of ferrites", *Proc. Brit. Ceramic Soc.*, vol. 2 (December 1964), p. 55.
10. H. M. O'Bryan *et al.*, "Microstructure control in nickel ferrous ferrite", *Amer. Ceram. Bull.*, vol. 48 (1969), p. 203.
11. J. C. M. de Lau, "Preparation of ceramic powders from sulphate solutions by spray-drying and roasting", *Amer. Ceram. Soc. Bull.*, vol. 49 (1970), p. 572.
12. F. J. Schnettler *et al.*, *Science of Ceramics*, vol. 4, edited by G. H. Stewart, Academic Press, London, 1968, p. 79.

13. *Final Report for Development of a Ferrite Material for a High Power Phase Shifter at S-band*, Airtron Device Laboratory, U.S. Gov. Res. Report No. AD433657, January 1964.
14. D. H. Harris, "Polycrystalline ferrite films for microwave applications deposited by arc-plasma", *J. Appl. Phys.*, vol. 41 (1970), p. 1348.
15. B. Bovarnick and H. W. Flood, *Method of Making Composite Materials and Resulting Products*, U.S. Patent No. 3305349, 1967.
16. H. B. Beer *et al.*, "Preparing ferrites by continuous electrolytic co-precipitation", *Brit. Comm. and Electronics*, vol. 15 (December 1958), p. 939.
17. R. L. Coble, "Sintering crystalline solids I and II", *J. Appl. Phys.*, vol. 32 (1961), pp. 787–92 and 793–799.
18. P. J. L. Reijnen, "Sintering behaviour and microstructures of aluminates and ferrites with spinel structure", *Sci. Ceram.*, vol. 4 (1968), p. 169.
19. B. Dobson and E. Rothwell, "Particle-size reduction in a fluid energy mill", *Powder Technology*, vol. 3 (1970), p. 213.
20. J. W. Nielsen and E. F. Dearborn, "Growth of Single Crystals of Magnetic Garnets," *J. Phys. Chem. Solids*, vol. 5, (1958), p. 202.
21. R. A. Laudise, "Technique of crystal growth", *J. Phys. Chem. Solids*, Suppl. 1 (1967), p. 3.
22. F. A. Reiss, "Automation of the verneuil process", *ibid.*, p. 63.
23. J. E. Mee *et al.*, "Magnetic oxide films", *Trans. I.E.E.E.*, MAG-5 (December 1969), p. 717.
24. T. Akashi *et al.*, "Preparation of ferrite single crystals by new floating zone technique", *Trans. I.E.E.E.*, MAG-5 (September 1969), p. 285.
25. Reference 3, chap. V.
26. C. Guillaud, "The properties of MnZn ferrites and the physical processes governing them", *Proc. I.E.E.*, 104B (1957), p. 165.
27. E. C. Snelling, *Soft Ferrites: Properties and Applications*, Iliffe Books Ltd, London, 1969, section 2.2.6.
28. L. G. van Uitert, "Dielectric properties and con-

ductivity in ferrites", *Proc. I.R.E.*, vol. 44 (1956), p. 1294.
29. G. B. Bogdanov, "Possible application of ferrites for solving problems in measurement technology", *Measurement Techniques (USSR)*, (January 1963), p. 33.
30. J. L. Snoek, "Effect of small quantities of carbon and nitrogen on the elastic and plastic properties of iron", *Physica*, vol. 8 (1941), p. 711.
31. S. Iida, "Mechanism of disaccommodation in ferrites", *J. Phys. Soc., Japan*, vol. 17 (1962), p. 123.
32. A. Fox, "Disaccommodation in manganese–zinc ferrite", *J. Phys. D.; Appl. Phys.*, vol. 4 (1971), p. 1239.
33. S. Krupička, "Study of relaxation spectrum of manganese ferrites", *J. Phys. Soc. Japan*, vol. 17 (1962), p. 304.
34. A. Broese van Groenou *et al.*, "Magnetism, microstructure and crystal chemistry of spinel ferrites", *Mater. Sci. Eng.*, vol. 3 (1968/69), p. 317.
35. J. G. M. de Lau, "Hot-pressed fine-grained ferrite properties", *Proc. Brit. Ceram. Soc.*, vol. 10 (1968), p. 275.
36. J. G. M. de Lau and A. L. Stuijts, "Chemical composition and high-frequency properties of Ni–Zn–Co ferrites", *Philips Res. Reps.*, vol. 21 (1966), p. 104.
37. J. G. M. de Lau, "Improvements of high-frequency properties of iron deficient Ni–Zn–Co ferrites by reduction of grain size", *Trans. I.E.E.E.*, MAG–5 (September 1969), p. 291.
38. A. Ikeda *et al.*, "Hot Pressed Ferrites and Magnetic Heads," Ferrites, Proceedings of the International Conf., July 1970. University Park Press (1971), p. 337.
39. A. L. Stuijts *et al.*, "Dense ferrites and their applications", *Trans. I.E.E.E., Comm. and Electr.*, vol. 83 (1964), p. 726.
40. R. D. Fisher *et al.*, "Single crystal ferrite materials for recording head applications", Ferrites, Proceedings

of the International Conf., July 1970. University Park Press (1971), p. 340.
41. K. Ohta, "Magnetocrystalline anisotropy and magnetic permeability of MnZn ferrous ferrite", *J. Phys. Soc., Japan*, vol. 18 (1963), p. 685.
42. E. Röss, "Magnetic properties and microstructure of High Permeability MnZn Ferrites," Ferrites, Proceedings of the International Conf., July 1970. University Park Press (1971), p. 203.
43. C. Guillaud *et al.*, "The reduction of eddy current losses in MnZn ferrites by the action of calcium", *C.R. Accad. Sci.* (Paris), vol. 242 (1956), p. 2712.
44. P. Mossman, "The effects of cooling conditions in the final firing cycle of manganese–zinc ferrite", Joint I.E.E./I.P.P.S. Conf. on Mag. Mats and their Appns., London, 26–28 September 1967, p. 164.
45. H. Jackson, "Kilns for the manufacture of ferrites", *Proc. Brit. Ceram. Soc.*, vol. 2 (December 1964), p. 43.
46. E. Röss and E. Moser, "The temperature dependence of initial permeability for high permeability MnZn ferrites", *Z. fur Angew Phys.*, vol. 13 (1961), p. 247.
47. T. G. W. Stijntjes *et al.*, "Permeability and conductivity of Ti-substituted MnZn ferrites", *Philips Res. Rep.*, vol. 25 (1970), p. 95.
48. Reference 3, chap. 14, section 51.
49. G. H. Jonker *et al.*, "Hexagonal ferromagnetic iron oxide compounds for very high frequencies", *Philips Res. Rep.*, vol. 18 (1963), p. 145.
50. T. Takada *et al.*, "A new preparation method of the Oriented Ferrite Magnets." Ferrites, Proceedings of the International Conf., July 1970. University Park Press (1971), p. 275.
51. P. B. Braun, "The crystal structure of a new group of ferrimagnetic compounds", *Philips Res. Rep.*, vol. 12 (1957), p. 491.
52. H. G. Richter, "On the magnetic properties of fine-milled barium and strontium ferrite", *Trans. I.E.E.E.*, MAG-4 (September 1968), p. 263.
53. A. Cochardt, "Recent ferrite magnet developments", *J. Appl. Phys.*, vol. 37 (1966), p. 1112.

54. A. Cochardt, "Effects of sulphates on the properties of strontium ferrite magnets", *J. Appl. Phys.*, vol. 38 (1967), p. 1904.
55. L. A. Russell *et al.*, "Ferrite memory systems", *Trans. I.E.E.E.*, MAG-4 (June 1968), p. 134.
56. L. V. Auletta *et al.*, "Ferrite core planes and arrays: IBM's manufacturing evolution", *Trans. I.E.E.E.*, MAG-5 (December 1969), p. 764.
57. R. S. Tebble and D. J. Craik, *Magnetic Materials*, J. Wiley and Sons Ltd., London, 1969, chap. 15.
58. A. P. Greifer, "Ferrite memory materials", *Trans. I.E.E.E.*, MAG-5 (December 1969), p. 774.
59. H. J. Williams *et al.*, "Stressed ferrites having rectangular hysteresis loops", *A.I.E.E. Trans. Comm. and Elect.*, vol. 72 (November 1953), p. 531.
60. P. K. Baltzer, "Effective magnetic anisotropy and magnetostriction of monocrystals", *Phys. Rev.*, vol. 108 (1957), p. 580.
61. J. B. Goodenough, "Chemical inhomogeneities and square B-H loops", *J. Appl. Phys.*, vol. 36 (1965), p. 2342.
62. H. P. J. Wijn *et al.*, "Conditions for square hysteresis loops in ferrites", *Philips Tech. Rev.*, vol. 16 (1954), p. 49.
63. A. H. Bobeck, "Properties and device applications of magnetic domains in orthoferrites", *B.S.T.J.*, vol. 46 (1967), p. 1901.
64. A. A. Thiele, "The theory of cylindrical magnetic domains", *B.S.T.J.*, vol. 48 (1969), p. 3287.
65. A. H. Bobeck *et al.*, "Applications of orthoferrites to domain-wall devices", *Trans. I.E.E.E.*, MAG-5 (1969), p. 544.
66. U. F. Gianola *et al.*, "Material requirements for circular magnetic domain devices", *Trans. I.E.E.E.*, MAG-5 (1969), p. 558.
67. A. H. Bobeck *et al.*, "Uniaxial Magnetic Garnets for Domain Wall 'Bubble' Devices", *Appl. Phys. Letts.*, vol. 17 (1970), p. 131.
68. D. M. Heinz, "Mobile cylindrical magnetic domains in epitaxial garnet films', *J. Appl. Phys.*, vol. 42 (1971), p. 1243.

69. E. Heinlein and R. D. Pierce, "Coercivity reduction in thin orthoferrite plates by annealing", *Trans. I.E.E.E.*, MAG-6 (September 1970), p. 493.
70. A. J. Perneski, "Propagation of cylindrical magnetic domains in orthoferrites", *Trans. I.E.E.E.*, MAG-5 (1969), p. 554.
71. P. I. Bonyhard *et al.*, "Applications of bubble devices", *Trans. I.E.E.E.*, MAG-6 (September 1970), p. 447.
72. B. Lax and K. J. Button, *Microwave Ferrites and Ferrimagnetics*, McGraw-Hill Book Co. Inc., 1962.
73. R. A. Waldron, *Ferrites: An Introduction for Microwave Engineers*, Van Nostrand Co. Ltd., London, 1961.
74. Reference 5, section I.6.
75. Q. H. F. Vrehen *et al.*, "Relaxation of ferromagnetic precession by excitation of spin waves in polycrystalline nickel–cobalt ferrites", *Phys. Rev.*, B1 (March 1970), p. 2332.
76. E. Schlomann, "Inhomogeneous broadening of ferromagnetic resonance lines", *J. Appl. Phys.*, vol. 40 (1969), p. 1199.
77. A. M. Clogston *et al.*, "Ferromagnetic resonance line width in insulating materials', *J. Phys. Chem. Solids*, vol. 1 (1956), p. 129.
78. M. Sparks, *Ferromagnetic Relaxation Theory*, McGraw-Hill Book Co. Inc., 1964.
79. M. Sparks, "Effect of impurities on the microwave properties of YIG", *J. Appl. Phys.*, vol. 38 (1967), p. 1031.
80. K. L. Kotzebue, "New trends in low-power ferrite limiters", *Electronics*, vol. 35, 21st December 1962, p. 40.
81. W. H. von Aulock and C. E. Fay, *Linear Ferrite Devices for Microwave Applications*, Academic Press, New York, 1968.
82. W. J. Ince and D. H. Temme, *Phasers and Time Delay Elements: Advances in Microwaves*, vol. 4, Academic Press Inc., New York, 1969.
83. W. J. Ince *et al.*, "The use of manganese-doped iron garnets and high-dielectric constant loading for

microwave latching ferrite phasers", 1970 Internat. Microwave Symposium Digest, p. 327.
84. B. Hershenov, "Miniature microstrip circulators using high-dielectric constant substrates", *R.C.A. Rev.*, vol. 30 (1969), p. 541.
85. R. H. Knerr *et al.*, "Compact, broad-band, thin film, lumped element circulator", *Trans. I.E.E.E.*, MTT–18 (1970), p. 1100.
86. M. E. Hines, "Reciprocal and non-reciprocal modes of propagation in ferrite stripline and microstrip devices", *Trans. I.E.E.*, MTT–19 (1971), p. 442.
87. U.S. Patent No. 3,555,459; 12th January 1971.
88. W. Venator, "Charting a simpler course to the design of YIG filters", *Electronics*, 3rd March 1969, p. 118.
89. M. Omari, "Octave electronic tuning of a CW Gunn diode using a YIG sphere", *Proc. I.E.E.E.* (*Letters*), vol. 57 (1969), p. 97.
90. D. H. Ridgley *et al.*, "Effects of lithium and oxygen losses on magnetic and crystallographic properties of spinel lithium ferrite", *J. Amer. Ceram. Soc.*, vol. 53 (1970), p. 304.
91. W. H. von Aulock, *Handbook of Microwave Ferrite Materials*, Academic Press Inc., New York, 1965.
92. E. E. Riches, "Advances in ferrite materials for microwave devices", *G.E.C. Jnl. of Science and Tech.*, vol. 35 (1968), p. 94.
93. C. E. Patton, "Effect of grain size on the microwave properties of polycrystalline YIG", *J. Appl. Phys.*, vol. 41 (1970), p. 1637.
94. L. R. Hodges *et al.*, "Temperature stability in yttrium–gadolinium aluminium–iron garnets", *J. Amer. Ceram. Soc.*, vol. 48 (1965), p. 516.
95. G. F. Dionne, *Magnetic Moment Versus Temperature Curves of Ferrimagnetic Garnet Materials*, Massachusetts Inst. of Tech., Lincoln Laboratory, Tech. Rep. 480, 9th September 1970.
96. A. E. Paladino and E. A. Maguire, "Microstructure development in yttrium iron garnet", *J. Amer. Ceram. Soc.*, vol. 53 (1970), p. 98.
97. S. Geller *et al.*, "Ferrimagnetic garnets containing

pentavalent vanadium", *J. Appl. Phys.*, vol. 35 (1964), p. 570.

98. P. Mossman, "The effect of processing conditions on the properties of Polycrystalline
$$Bi_{3-2x}Ca_{2x}Fe_2Fe_{3-x}V_xO_{12}$$
ferrites", *Trans. I.E.E.E.*, MAG–5 (1969), p. 614.
99. H. J. van Hook *et al.*, "Linewidth reduction through indium substitution in calcium–vanadium garnets", *J. Appl. Phys.*, vol. 39 (1968), p. 730.
100. G. F. Dionne, "Magnetic anisotropy and magnetostriction constants of MgMn ferrites at 300K", *J. Appl. Phys.*, vol. 41 (1970), p. 831.
101. Reference 3, chap. 9.
102. G. P. Rodrigue, "Magnetic materials for millimeter wave applications", *Trans. I.E.E.E.*, MTT–11 (1963), p. 351.
103. A. M. Clogston *et al.*, "Possible source of linewidth in ferrimagnetic resonance", *Phys. Rev.*, vol. 101 (1956), p. 903.
104. E. Schlomann *et al.*, "Generation of spin waves in nonuniform magnetic fields, with application to magnetic delay lines", *Proc. I.E.E.E.*, vol. 53 (1965), p. 1495.
105. M. F. Lewis, "Ultrasonics and spin waves in microwave delay lines", *GEC–AEI Jnl. of Sc. and Tech.*, vol. 35 (1968), p. 99.
106. I. N. Court, "Microwave acoustic devices for pulse compression filters", *Trans. I.E.E.E.*, MTT–17 (19 69), p. 968.
107. J. H. Collins, "Microwave integrated circuits utilizing Epitaxial YIG Films," Ferrites, Proceedings of the International Conf., July 1970. University Park Press (1971), p. 487.
108. Reference 3, chap. 4, section 13.2, and chap. 8, section 35.
109. C. M. van der Burgt, "Ferrocube material for piezomagnetic vibrators", *Philips Tech. Rev.*, vol. 18 (1956/57), p. 285.
110. Y. Kikuchi, "Magnetostrictive materials and applications", *Trans. I.E.E.E.*, MAG–4 (1968), p. 107.

INDEX

The Author

Eric E. Riches received the B.Sc. degree in physics and mathematics in 1948 and the M.Sc. in mathematics in 1950, both from the University of London.

From that time he has worked at the Hirst Research Laboratories of the General Electric Co. Ltd. on research and development in various areas of physics closely associated with electronics and electrical engineering.

Up to 1954 he did research on the dielectric and piezoelectric applications of ferroelectrics, and from 1955 to 1960 he led a section researching into h.f. cables and interference from power systems. This was followed by a period on thin-film magnetic memory-store circuitry. Since 1962 he has led a group working on magnetic ceramics and microwave ferrite devices, and is now also responsible for research into other problems in applied magnetics. He is a Member of the Institute of Physics.

Mills & Boon Ltd
17-19 Foley Street, London W1A 1DR